Investigation of long-wave model equations for a liquid CO_2-seawater interface in deep water

Master thesis in applied and computational mathematics

Krister Joakim Trandal

Department of Mathematics
University of Bergen
October 2, 2017

Acknowledgments

First and foremost I would like to thank my supervisor, professor Henrik Kalisch, for his motivational discussions and instruction, in a welcoming atmosphere, for the making of this thesis.

Further I would like to thank Daulet Moldabayev for his fruitful inputs on running the `SpecTraVVave` package.

Last but certainly not least, thanks to my family for their patience and support, giving me the opportunity to pursue many years of study, and to friends for making those years in Bergen as memorable as possible.

Krister J. Trandal,
Bergen, October 2017

Outline and motivation

In this work, we will take a detailed look at some internal wave models, both linear and nonlinear, where the waves propagate on a fluid interface and are subjected to capillarity. After presenting the prerequisites, a detailed derivation of the evolution equations is given. A model equation restricted to unidirectional wave propagation between seawater and carbon dioxide (CO_2) will then be studied numerically in its own independent article. The work is partly motivated by previously conducted deep ocean experiments studying the stability of the interface between seawater and a submerged pool of CO_2 [9]. Numerical bifurcation analysis is used to study the response of the system to various imposed shear flows. The thesis is structured as follows.

In the introductory Chapter 1 we review some fundamental concepts and laws of fluid mechanics, and put forward the assumptions about the fluids and flow fields that are employed throughout the paper.

In Chapter 2 we describe the fluid interface problem with imposed shear flow. The treatment is kept at a general level with all spatial dimensions included, and the obtained formulation serves as a basis for the subsequent derivations of model equations under more restrictive suppositions. Further, we take a look at the linear dispersion relation. The chapter closes with a derivation of solitary wave solutions of the Korteweg-de Vries equation.

In Chapter 3 an overview of some mathematical ingredients that are employed subsequently in the paper are given. Of notable importance is the so-called Hilbert transform and some of its properties, and how it is used in solving an upper half-plane Neumann problem arising in our later derivations. The chapter is not meant to be a comprehensive treatise on the results presented, but rather to serve as a preamble for what is to come.

In Chapter 4 the general derivation of the nonlinear evolution equations is given, employing nondimensionalization and formal asymptotic expansions to arrive at the desired results. The theory of Chapter 3 is used extensively. Finally, we connect the linearized model equations with the dispersion relations from Chapter 2.

In Chapter 5 our independent article is presented in its entirety, which encompasses the numerical analysis of a nonlinear model equation. The derivation of the equation is essentially a specialization of that presented in Chapter 4, restricting wave propagation to one spatial dimension.

Contents

Chapter 1

Introduction

1.1 Fluid mechanics

A satisfactory and comprehensive description of fluid flow phenomena involves several conservation laws and equations of state. As noted in [16, pp. 355-357], one can end up with over twenty equations in equally many variables. The goal here is obviously not to go through all such developments that are found in books on continuum and fluid mechanics.

We will only cover what we believe is necessary to make the current paper complete, our treatment being tailored to suit the needs of later chapters. In this section we will present some terminology and assumptions that are made about the fluids and the flow field.

Viscosity

Viscosity is a measure of the "internal friction" or resistance to shear stress in the fluid, and is present in nearly all real fluids [14, p. 562]. The viscosity is usually a function of the thermodynamic state, and for most fluids it displays a significant dependence on temperature. An informal characterization of viscosity is the "thickness" of the fluid; blood has higher viscosity than water[1]. Throughout this paper, we will assume that viscous effects in fluids are negligible. This is generally a reasonable assumption far from solid boundaries, where thin viscous boundary layers are usually present [4, p. 104].

Incompressible fluids and irrotational flow

A fluid in which the density ρ is a function of pressure p only is said to be *barotropic*. In the special case when ρ is a constant function of pressure, the fluid is called *incompressible* [4, p. 118]. A fluid flow is termed *irrotational* if the vorticity vector $\boldsymbol{\omega}$ vanishes throughout

[1] In accordance with the proverb.

the flow domain. That is,

$$\boldsymbol{\omega} := \nabla \times \mathbf{u} = \mathbf{0}, \tag{1.1}$$

where $\mathbf{u}$ denotes the velocity field. The vorticity measures the local rotation of fluid elements, and is precisely equal to twice the angular velocity of such rotation. If the flow is irrotational, it is not difficult to demonstrate that the velocity field $\mathbf{u}$ can be written in terms of a potential function ϕ, that is,

$$\mathbf{u} = \nabla\phi. \tag{1.2}$$

As will be seen later, this is quite convenient, one reason being that it is easier to work with the scalar potential ϕ rather than the velocity field $\mathbf{u}$ itself.

A quantity related to the vorticity is the *circulation* in a fluid, defined by [4, p. 63-64]

$$\Gamma = \oint_C \mathbf{u} \cdot \mathbf{ds} = \oint_A (\nabla \times \mathbf{u}) \cdot \mathbf{dA} = \oint_A \boldsymbol{\omega} \cdot \mathbf{dA}, \tag{1.3}$$

the second equality being due to Stokes' theorem, and the final equality from using the definition of $\boldsymbol{\omega}$. A fundamental result regarding the circulation Γ which we will make use of later is Kelvin's circulation theorem. This states that the circulation around a material contour moving with the fluid remains constant with time, under the assumption that the flow be barotropic and inviscid, with only conservative body forces (like gravity) acting on the fluid. This can be stated mathematically as [4, p. 144-145]

$$\frac{D\Gamma}{Dt} = 0, \tag{1.4}$$

where $\frac{D}{Dt}$ is the material time derivative (see Section 1.3). A corollary of this theorem is the fact that under the restrictions posed, irrotational flows remain irrotational [4, p. 148].

Dimensionless quantities

As is most likely familiar from our everyday experience, fluid flow phenomena can be complex: the waves and whirls in the ocean, or the air flowing over a moving vehicle. Consequently, attempting to describe such behavior mathematically can be a challenging endeavor.

In certain cases, a qualitative description can be achieved with the use of certain dimensionless parameters. Among the many that are used in fluid mechanics, perhaps the most prominent is the *Reynolds number*

$$\mathrm{Re} := \frac{UL}{\nu} \tag{1.5}$$

where U and L are characteristic velocity and length scales, respectively, and ν is the kinematic viscosity. Dimensionless quantities like the Reynolds number often occur when

the equations of interest are put in nondimensional form [4, pp. 279-284]. From a more practical standpoint, the Reynolds number can elucidate the dynamic similarities between flows that occur on different length scales, like the model aircraft in a wind tunnel compared to the real life version.

In this work, we will not work explicitly with the Reynolds number, but we will be interested in a different dimensionless parameter, the so-called *Bond number*, defined as [4, p. 289]

$$\text{Bo} := \frac{\rho g L^2}{\tau}, \tag{1.6}$$

where g is the acceleration of gravity, and τ is the surface tension parameter (see the next section). The Bond number is important when one wants to consider how surface tension effects balance those of gravity.

1.2 Surface tension and capillarity

The interface between two immiscible fluids, for instance the free surface between air and water, acts as if it were under tension, similar to that of a stretched membrane [4, p. 8], [14, p. 455]. The nature and origin of this surface tension is explained on the molecular levels. For the sake of simplicity and familiarity, assume the fluids are water and air. Molecules that comprise the interface will be pulled unequally due to the different fluids. The water molecules in this case will be pulling more on the interface, and it therefore tends to curve. Surface tension effects explain why water droplets and bubbles in water tend to be of spherical shape [4, p. 8].

To be more precise, surface tension, denoted here and subsequently with the variable τ, can be defined as the amount of tensile force per unit length, with SI units N/m [4, pp. 8-9]. We now desire to derive a relationship between surface tension and the pressure difference across a curved interface.

Consider an arc element ds of the fluid interface denoted by η between two immiscible fluids, with pressures measured close to the interface denoted by p_1 and p_2 (see Figure 1.1). The interface arc element is assumed to be extended a unit of one meter in the transverse direction, i.e. into the paper. Forces due to surface tension act on the endpoints of the arc, and their total contribution in the direction orthogonal to the arc is of interest. The contribution from the surface tension forces is shown schematically in Figure 1.2. The force $F_{\tau,n}$ is the contribution of $F_\tau = \tau \cdot 1$ in the direction normal to the interface, and is given by

$$F_{\tau,n} = F_\tau \cdot \sin\left(\frac{d\theta}{2}\right) = \tau \cdot \sin\left(\frac{d\theta}{2}\right) \approx \tau \cdot \frac{d\theta}{2}, \tag{1.7}$$

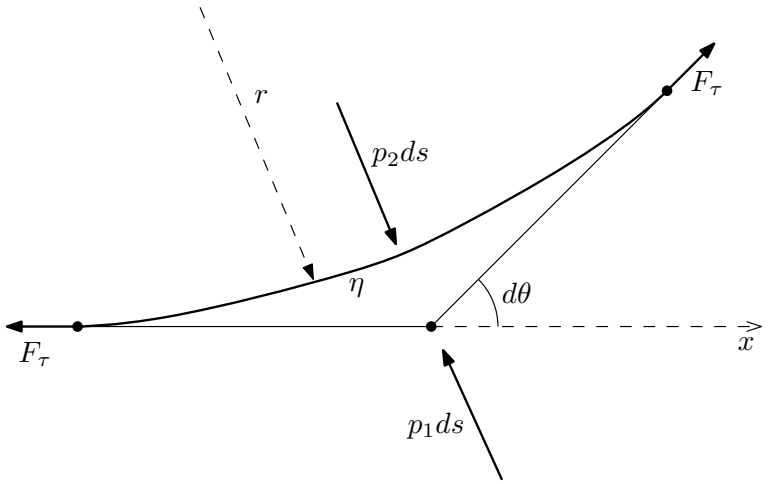

Figure 1.1: Force contribution of pressure and surface tension on a fluid surface arc element ds.

where the approximate equality holds for small angles $\frac{d\theta}{2}$. A force balance in the direction orthogonal to the interface η yields

$$p_1 ds + 2F_{\tau,n} - p_2 ds = p_1 ds + \tau d\theta - p_2 ds = 0. \tag{1.8}$$

This may be rewritten as

$$\tau \frac{d\theta}{ds} = p_2 - p_1 \tag{1.9}$$

Now, from elementary differential geometry, the curvature κ of the arc is given by

$$\kappa := \frac{1}{r} = \frac{d\theta}{ds} = \frac{\eta_{xx}}{\{1 + \eta_x^2\}^{3/2}} \approx \eta_{xx}, \tag{1.10}$$

where we have assumed that the slope η_x is small, in order to arrive at the final result. We thereby get

$$p_2 - p_1 = \tau \eta_{xx}. \tag{1.11}$$

When surface tension has notable influence on fluid behavior, the term *capillarity* is often used in relation to the phenomena being described. In this work, we will be looking at internal water waves subject to both capillarity and gravity, and such waves are then naturally termed capillary-gravity waves. However, we shall not be too much concerned with the interface between air and water, but rather between two arbitrary fluids with differing but constant densities.

We will then later look at the case where the two fluids involved are seawater and carbon dioxide (CO_2). For this reason, we will use the more appropriate terminology *interfacial tension* rather than surface tension in later chapters, to emphasize that the situation under study involves a more general fluid interface, and not necessarily a free surface like that between water and air.

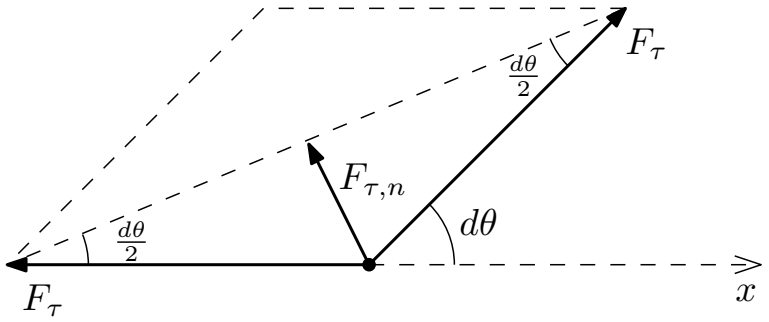

Figure 1.2: Decomposition of surface tension force contributions. The angle $d\theta$ is assumed to be small.

1.3 Bernoulli equation

From a cornerstone conservation law of fluid mechanics, the Navier-Stokes momentum equation, one may derive various simplified models under certain assumptions on the fluid and the flow field. The derivation presented is based on that given in [4, pp. 118-121].

We are especially interested in the case where the fluid is barotropic, that is, when density is a function of pressure only, $\rho = \rho(p)$, and the flow is inviscid, incompressible and irrotational. When viscosity is negligible, the incompressible Navier-Stokes equation

$$\rho \frac{D\mathbf{u}}{Dt} = -\nabla p + \rho \mathbf{g} + \mu \nabla^2 \mathbf{u} \tag{1.12}$$

reduces to the *Euler equation*

$$\rho \frac{D\mathbf{u}}{Dt} = -\nabla p + \rho \mathbf{g}, \tag{1.13}$$

where we assume that gravity is the only body force acting on the fluid. The differential operator $\frac{D}{Dt} := \frac{\partial}{\partial t} + \mathbf{u} \cdot \nabla$ denotes the material time derivative. That is, the time derivative following a material fluid particle expressed in Eulerian variables. In component form, equation (1.13) becomes

$$\frac{\partial u_i}{\partial t} + u_j \frac{\partial u_i}{\partial x_j} = -\frac{\partial}{\partial x_i}(g x_3) - \frac{1}{\rho}\frac{\partial p}{\partial x_i}. \tag{1.14}$$

where terms with repeated indices enforce the summation convention. The second term on the left of (1.14) may be rewritten as

$$\begin{aligned} u_j \frac{\partial u_i}{\partial x_j} &= u_j \left(\frac{\partial u_i}{\partial x_j} - \frac{\partial u_j}{\partial x_i} \right) + u_j \frac{\partial u_j}{\partial x_i} = u_j r_{ij} + \frac{\partial}{\partial x_i}\left(\frac{1}{2} u_j^2\right) \\ &= -u_j \varepsilon_{ijk} \omega_k + \frac{\partial}{\partial x_i}\left(\frac{1}{2} u_j^2\right) = -(\mathbf{u} \times \boldsymbol{\omega})_i + \frac{\partial}{\partial x_i}\left(\frac{1}{2} u_j^2\right) \end{aligned}$$

where R_{ij} are the components of the rotation tensor[2]. The relationship $u_j R_{ij} = -u_j \varepsilon_{ijk} \omega_k$ follows once it is recognized that the rotation tensor R_{ij} and the vorticity vector $\boldsymbol{\omega} = (\omega_1, \omega_2, \omega_3)$ are related through

$$R = \begin{pmatrix} 0 & -\omega_3 & \omega_2 \\ \omega_3 & 0 & -\omega_1 \\ -\omega_2 & \omega_1 & 0 \end{pmatrix}$$

Now, since the flow is assumed to be barotropic, we have that [4, p. 118]

$$\frac{1}{\rho} \frac{\partial p}{\partial x_i} = \frac{\partial}{\partial x_i} \int \frac{dp}{\rho}.$$

The Euler equation (1.14) becomes

$$\frac{\partial u_i}{\partial t} + \frac{\partial}{\partial x_i} \left(\frac{1}{2} u_j^2 + \int \frac{dp}{\rho} + g x_3 \right) = (\mathbf{u} \times \boldsymbol{\omega})_i. \tag{1.15}$$

When the flow is irrotational, the vorticity $\boldsymbol{\omega}$ vanishes, and we can write the velocity field $\mathbf{u}$ in terms of a potential function ϕ: $\mathbf{u} = \nabla \phi$. This leads to

$$\nabla \left(\phi_t + \frac{1}{2} u_j^2 + \int \frac{dp}{\rho} + g x_3 \right) = 0, \tag{1.16}$$

which implies that

$$\phi_t + \frac{1}{2} u_j^2 + \int \frac{dp}{\rho} + g x_3 = F(t). \tag{1.17}$$

The function $F(t)$ may be incorporated into the function ϕ_t by a suitable transformation, e.g.

$$\phi \mapsto \phi - \int_{t_0}^{t} F(\nu) d\nu, \tag{1.18}$$

and applying the fundamental theorem of calculus. Reminding ourselves that the flow is assumed to be incompressible, ρ will be a constant function of pressure, and from equations (1.17) and (1.18), we finally obtain our desired form of a Bernoulli equation:

$$\phi_t + \frac{1}{2} u_j^2 + \frac{p}{\rho} + g x_3 = 0. \tag{1.19}$$

[2]The velocity gradient tensor $\nabla \mathbf{u}$ can be written as a sum of symmetric and antisymmetric tensors; the antisymmetric part corresponds to the rotation tensor R_{ij} (cf. [4, pp. 40-41]).

Chapter 2

Water wave theory

In this outset analysis, we formulate the fluid interface problem with imposed uniform shear flow, which is well known for exhibiting Kelvin-Helmholtz instability. One goal is to arrive at a linear formulation of the field equations and boundary conditions, and proceed to derive a linear dispersion relation. We will then revisit some of these dispersion relations in Chapter 4, in connection with the nonlinear model equations.

2.1 Fluid interface waves

Our problem of study involves a system of two fluids, separated by a sharp density interface denoted by $z = \eta(x, y, t)$. As suggested from the notation, we will keep the initial treatment general and include all spatial dimensions x, y and z in a standard Cartesian coordinate system[1]. The variable t denotes time. See Figure 2.1 for a depiction. The subsequent developments are similar to those found in [4, pp. 493-496].

The total flow in each layer is regarded as a superposition of the imposed uniform background flow and the perturbed flow arising from the interface disturbance (cf. [6, pp.]). Before the interface is disturbed, the flow is solely steady and uniform, and consequently irrotational. Kelvin's circulation theorem (see eq. (1.4)) guarantees that it remains so. We can then write the total flow in each layer in terms of the potentials ϕ' and ψ':

$$\phi' = U_1 x + \phi, \tag{2.1}$$

$$\psi' = U_2 x + \psi, \tag{2.2}$$

where ϕ and ψ denote the velocity potentials of the perturbed flow. It follows from the

[1] Although the problem is three-dimensional, we will refer to the wave propagation and corresponding model equations as either one-dimensional (in the spatial variable x) or two-dimensional (in the spatial variables x, y). It is to be understood that the vertical coordinate z and time t are always included.

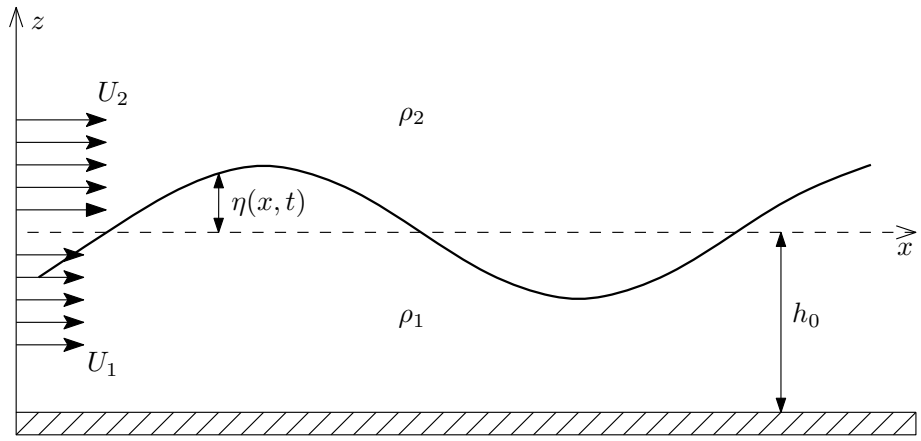

Figure 2.1: Geometry of the fluid interface problem. The upper layer (index 2) is assumed to be infinitely deep, while the lower layer (index 1) has a finite depth h_0 measured from the undisturbed interface located at $z = 0$. The variables ρ_1 and ρ_2 denote the densities of the lower and upper layers, respectively. In both layers there is an imposed uniform shear flow, U_1 and U_2, in the x direction. We further assume that $\rho_2 < \rho_1$.

incompressible continuity equation[2] that ϕ' and ψ' must satisfy Laplace's equation in the respective layers. It is then immediate that ϕ and ψ, which are the primary unknowns, must also each satisfy Laplace's equation. Thus, the governing field equations are

$$\triangle\phi = 0, \quad -h_0 < z < \eta, \tag{2.3}$$

$$\triangle\psi = 0, \quad \eta < z < \infty, \tag{2.4}$$

with boundary conditions

$$\phi_x = 0, \quad \phi_y = 0, \quad \phi_z = 0, \text{ at } z = -h_0, \tag{2.5}$$

$$\psi_x \to U_2, \quad \psi_y \to 0, \quad \psi_z \to 0 \text{ as } z \to +\infty, \tag{2.6}$$

and

$$\left.\begin{aligned} \mathbf{n}\cdot\nabla\phi' = \mathbf{n}\cdot\nabla(U_1 x + \phi) &= \mathbf{n}\cdot\mathbf{u}_s, && (2.7)\\ \mathbf{n}\cdot\nabla\psi' = \mathbf{n}\cdot\nabla(U_2 x + \psi) &= \mathbf{n}\cdot\mathbf{u}_s, && (2.8)\\ p_2 - p_1 &= \tau\eta_{xx}, && (2.9) \end{aligned}\right\} \text{ at } z = \eta.$$

In the last expressions, $\mathbf{n}$ is the local unit normal at the interface, $\mathbf{u}_s$ is the velocity of the interface, p_1 and p_2 are the pressures in each layer, and τ is a positive parameter known as the interfacial surface tension. The conditions in equation (2.5) are the no-slip and no-flow-through boundary conditions. The expressions in equation (2.6) states that the velocity field

[2]The incompressible continuity equation, $\nabla\cdot\mathbf{u} = 0$, concerns the principle of mass conservation, and is necessary alongside the momentum equation to give an adequate description of fluid flows.

should remain uniform far from the fluid interface. Equations (2.7) and (2.8) are kinematic conditions stating that the velocities in each layer at the interface must match the velocity of the interface itself. The final dynamic condition (2.9) relates the pressure difference to the interfacial tension (see Section 1.2). Letting $f(x,y,z,t) = z - \eta(x,y,t)$, we can calculate $\mathbf{n}$ as

$$\mathbf{n} = \frac{\nabla f}{|\nabla f|} = \frac{\left(-\eta_x \mathbf{e}_x - \eta_y \mathbf{e}_y + \mathbf{e}_z\right)}{\left\{1 + \eta_x^2 + \eta_y^2\right\}^{1/2}}, \quad z = \eta.$$

Assuming pure vertical interface velocity $\mathbf{u}_s = \eta_t \mathbf{e}_z$, we have from eqs. (2.7) and (2.8) that

$$\mathbf{n} \cdot \nabla \phi' = \frac{-(U_1 + \phi_x)\eta_x - \phi_y \eta_y + \phi_z}{\left\{1 + \eta_x^2 + \eta_y^2\right\}^{1/2}} = \frac{\eta_t}{\left\{1 + \eta_x^2 + \eta_y^2\right\}^{1/2}}, \quad z = \eta,$$

$$\mathbf{n} \cdot \nabla \psi' = \frac{-(U_2 + \psi_x)\eta_x - \psi_y \eta_y + \psi_z}{\left\{1 + \eta_x^2 + \eta_y^2\right\}^{1/2}} = \frac{\eta_t}{\left\{1 + \eta_x^2 + \eta_y^2\right\}^{1/2}}, \quad z = \eta,$$

or

$$-\left(U_1 + \phi_x\right)\eta_x - \phi_y \eta_y + \phi_z = \eta_t = -\left(U_2 + \psi_x\right)\eta_x - \psi_y \eta_y + \psi_z, \quad z = \eta. \tag{2.10}$$

For pressure, we have the following Bernoulli equations (see eq. (1.19)):

$$\phi_t' + \frac{1}{2}\left|\nabla \phi'\right|^2 + \frac{p_1}{\rho_1} + gz = C_1, \quad z = \eta. \tag{2.11}$$

$$\psi_t' + \frac{1}{2}\left|\nabla \psi'\right|^2 + \frac{p_2}{\rho_2} + gz = C_2, \quad z = \eta. \tag{2.12}$$

Applying eqs. (2.11), (2.12) to the dynamic condition (2.8), keeping in mind the expressions (2.1) and (2.2), we get

$$\begin{aligned} p_2 - p_1 &= \rho_2\left(C_2 - \psi_t' - \frac{1}{2}\left|\nabla \psi'\right|^2 - g\eta\right) - \rho_1\left(C_1 - \phi_t' - \frac{1}{2}\left|\nabla \phi'\right|^2 - g\eta\right) \\ &= \rho_2\left(C_2 - \psi_t - \frac{1}{2}U_2^2 - U_2\psi_x - \frac{1}{2}|\nabla\psi|^2 - g\eta\right) \\ &\qquad - \rho_1\left(C_1 - \phi_t - \frac{1}{2}U_1^2 - U_1\phi_x - \frac{1}{2}|\nabla\phi|^2 - g\eta\right) \\ &= \rho_1\left(\phi_t + U_1\phi_x + \frac{1}{2}|\nabla\phi|^2 + g\eta\right) - \rho_2\left(\psi_t + U_2\psi_x + \frac{1}{2}|\nabla\psi|^2 + g\eta\right) = \tau\eta_{xx}, \end{aligned} \tag{2.13}$$

at $z = \eta$. The second to last equality arises from the fact that in the undisturbed state, with $\phi = \psi = 0$ and $\eta = 0$ the pressure must be continuous, so we require that [4, p. 495]

$$(p_1)_{\text{undisturbed}} = \rho_1\left(C_1 - \frac{1}{2}U_1^2\right) = \rho_2\left(C_2 - \frac{1}{2}U_2^2\right) = (p_2)_{\text{undisturbed}}\,.$$

Linearization

Condition (2.10) can be linearized by neglecting higher order terms, and evaluating derivatives at $z = 0$ instead of at $z = \eta$ using a Taylor expansion [4, pp. 220-221]. We thereby obtain

$$-U_1\eta_x + \phi_z = \eta_t = -U_2\eta_x + \psi_z, \quad z = 0. \tag{2.14}$$

Similarly, the dynamic condition (2.13) can be linearized about $z = 0$ to give

$$\rho_1\left(\phi_t + U_1\phi_x + g\eta\right) - \rho_2\left(\psi_t + U_2\psi_x + g\eta\right) = \tau\eta_{xx}, \quad z = 0. \tag{2.15}$$

2.2 Dispersion relation

To solve the Laplace problems (2.3), (2.4) subject to the conditions (2.5), (2.6), (2.14) and (2.15), we apply the method of normal modes [4, pp. 469-470] and assume a sinusoidal waveform in each layer when the interface is disturbed:

$$\phi(x,z,t) = A_1(z)e^{ik(x-ct)}, \quad \psi(x,z,t) = A_2(z)e^{ik(x-ct)}.$$

Substitution into the Laplace equations and dividing out the exponential factor results in the two ODEs

$$\frac{dA_1}{dz} - k^2A_1 = 0, \quad \frac{dA_2}{dz} - k^2A_2 = 0,$$

whose general solutions are found to be

$$A_1(z) = a_1e^{|k|z} + b_1e^{-|k|z}, \quad A_2(z) = a_2e^{|k|z} + b_2e^{-|k|z}.$$

With the conditions given in (2.5) and (2.6), we require that $a_2 = 0$ and $b_1 = a_1e^{-2|k|h_0}$.

Now apply the linearized kinematic condition (2.14) to determine a_1 and b_2. We assume an interfacial shape of the form $\eta(x,t) = \eta_0e^{ik(x-ct)}$, and thereby obtain

$$\begin{aligned} -U_1ik\eta_0e^{ik(x-ct)} + a_1|k|(e^{|k|z} - e^{-|k|z-2|k|h_0})e^{ik(x-ct)} &= -\eta_0ikce^{ik(x-ct)} \\ &= -U_2ik\eta_0e^{ik(x-ct)} - b_2|k|e^{ik(x-ct)-|k|z}, \end{aligned}$$

or

$$-U_1ik\eta_0 + a_1|k|(e^{|k|z} - e^{-|k|z-2|k|h_0}) = -ikc\eta_0 = -U_2ik\eta_0 - b_2|k|e^{-|k|z},$$

which, at $z = 0$, simplifies to

$$-U_1ik\eta_0 + a_1|k|(1 - e^{-2|k|h_0}) = -ikc\eta_0 = -U_2ik\eta_0 - b_2|k|.$$

Hence

$$a_1 = i\,\eta_0\frac{U_1 - c}{1 - e^{-2kh_0}}\mathrm{sgn}(k), \quad b_2 = i\,\eta_0(c - U_2)\mathrm{sgn}(k).$$

Now substitute the expressions for ϕ, ψ and η into the linearized dynamic condition (2.15) to obtain, after some algebraic manipulations, a quadratic equation in the wave speed c:

$$\begin{aligned}(2.16)\quad &\left\{\rho_1 k\coth(kh_0)+\rho_2|k|\right\}c^2-\left\{2\rho_1 kU_1\coth(kh_0)+2\rho_2U_2|k|\right\}c\\ &+\left\{\rho_1U_1^2k\coth(kh_0)+\rho_2U_2^2|k|+(\rho_2-\rho_1)g-\tau k^2\right\}=0.\end{aligned}$$

Solving this equation for c, we extract the following linear dispersion relation:

$$\begin{aligned}(2.17)\qquad c(k)=&\frac{\rho_1U_1k\theta+\rho_2U_2|k|}{\rho_1k\theta+\rho_2|k|}\pm\frac{1}{\rho_1k\theta+\rho_2|k|}\\ &\cdot\left\{\tau k^2(\rho_1k\theta+\rho_2|k|)-\rho_1\rho_2(U_1-U_2)^2k|k|\theta+(\rho_1-\rho_2)(\rho_1k\theta+\rho_2|k|)g\right\}^{1/2},\end{aligned}$$

where $\theta=\coth(kh_0)$.

Long-wave and short-wave approximations

One can obtain a long-wave or shallow water approximation of the above dispersion relation (2.16). In this case, k will be small[3], and from the expansion of the hyperbolic function in its argument, we find that

$$(2.18)\qquad (kh_0)\coth(kh_0)=1+\frac{(kh_0)^2}{3}+\mathcal{O}\left((kh_0)^3\right)\approx 1,$$

where the approximate equality holds for small kh_0. So the long-wave approximation to the dispersion relation (2.16) is

$$\begin{aligned}(2.19)\qquad &\left\{\rho_1+\rho_2h_0|k|\right\}c^2-\left\{2\rho_1U_1+2\rho_2h_0U_2|k|\right\}c\\ &+\left\{\rho_1U_1^2+\rho_2h_0U_2^2|k|+(\rho_2-\rho_1)h_0g-h_0\tau k^2\right\}=0.\end{aligned}$$

For the opposite scenario, the short-wave or deep water approximation, the wave number k is large. In a similar argument to that given in (2.18), the hyperbolic function $\coth(kh_0)$ may be replaced by unity to give

$$\begin{aligned}(2.20)\qquad &\left\{\rho_1k+\rho_2|k|\right\}c^2-\left\{2\rho_1U_1k+2\rho_2U_2|k|\right\}c\\ &+\left\{\rho_1U_1^2k+\rho_2U_2^2|k|+(\rho_2-\rho_1)g-\tau k^2\right\}=0,\end{aligned}$$

which is the short-wave approximation to (2.16). The corresponding wave speed solutions for the two cases can be extracted from (2.17) by applying the appropriate approximations just described.

[3]In shallow water, h_0 is small. Throughout this study, we are assuming that the undisturbed lower layer depth h_0 is fixed.

2.3 Exact solution of a KdV-type equation

From our discussion of linear wave theory, we take a leap to look briefly at a nonlinear model equation, which is taken up again later chapters. The Korteweg-de Vries (KdV) equation, commonly written in the dimensionless form

$$u_t + 6uu_x + u_{xxx} = 0 \tag{2.21}$$

is well known for being an exactly solvable model equation describing the evolution of unidirectional long-crested waves on a shallow water surface [5, pp. 1-16]. As we will see in Chapter 5, the derived model equation for long waves on a density interface reduces to a KdV-type equation when the upper layer shear velocity attains a certain value.

In light of this, we desire the exact solution, which is used to test the numerical implementation carried out later on. The subsequent derivation of solitary wave solutions of the KdV equation is based on the material presented in [5, pp. 20-22].
When $U = c_0 v_0$ in eq. (**??**), we obtain (writing u in place of η)

$$u_t + u_x + \frac{3}{2}uu_x - \gamma u_{xxx} = 0, \tag{2.22}$$

with

$$\gamma = \frac{1}{2}\frac{\tau}{(\rho_1 - \rho_2)gh_0^2} > 0.$$

We seek traveling wave solutions of (2.22), i.e. solutions in the form

$$u(x,t) = w(z), \quad z = x - ct.$$

Substitution into (2.22) produces the ODE

$$-c\frac{dw}{dz} + \frac{dw}{dz} + \frac{3}{2}w\frac{dw}{dz} - \gamma\frac{d^3w}{dz^3} = -c\frac{dw}{dz} + \frac{dw}{dz} + \frac{3}{4}\frac{d}{dz}\left(w^2\right) - \gamma\frac{d^3w}{dz^3} = 0.$$

This can be integrated once to give

$$(1-c)w + \frac{3}{4}w^2 - \gamma\frac{d^2w}{dz^2} = E_1,$$

where E_1 is a constant of integration. We can now use w' as an integrating factor. Then, from a second integration we get

$$\frac{1}{2}(1-c)w^2 + \frac{1}{4}w^3 - \frac{1}{2}\gamma\left(\frac{dw}{dz}\right)^2 = E_1 w + E_2,$$

or

$$\gamma\left(\frac{dw}{dz}\right)^2 = \frac{1}{2}w^3 + (1-c)w^2 - 2(E_1 w + E_2). \tag{2.23}$$

We require our solutions to be real and bounded, so we must have that

$$f(w) := \frac{1}{2}w^3 + (1-c)w^2 - 2(E_1 w + E_2) \geq 0.$$

Posing the asymptotic conditions w, $\frac{dw}{dz}$, $\frac{d^2w}{dz^2} \to 0$ as $z \to \pm\infty$, leads to $E_1 = E_2 = 0$ and

$$f(w) = w^2\left(\frac{1}{2}w + (1-c)\right) \geq 0.$$

Equation (2.23) can be written as

$$\frac{dw}{w\left(\frac{1}{2}w + (1-c)\right)^{1/2}} = \pm\sqrt{\frac{1}{\gamma}}dz.$$

Assuming $0 < c < 1$, and using the substitution $w = 2(c-1)\operatorname{sech}^2\theta$, results in

$$\frac{-2}{\sqrt{1-c}}\int d\theta = \pm\sqrt{\frac{1}{\gamma}}\int dz.$$

Consequently, our traveling wave solution takes the form

$$u(x,t) = w(x-ct) = 2(c-1)\operatorname{sech}^2\left(\frac{1}{2}\sqrt{\frac{1-c}{\gamma}}(x-ct-x_0)\right), \tag{2.24}$$

where x_0 is an arbitrary constant corresponding to a phase shift. A plot of the solution (2.24) with $c = 0.5$ is given below.

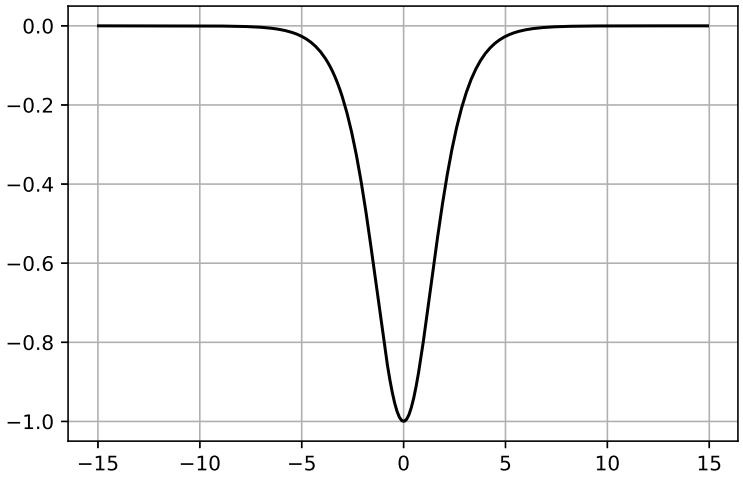

Figure 2.2: Solitary wave solution of the KdV equation with $c = \frac{1}{2}$. We see that in our case the profile is a wave of depression, for any admissible value of c between 0 and 1.

Chapter 3

Mathematical theory

The intention in this chapter is to review some mathematical concepts that is used throughout the rest of the paper. It is by no means meant to be a comprehensive treatment of the respective subjects, but rather to serve as an overview and a place for reference.

3.1 The Fourier and Hilbert transforms

An integral transform known as the *Hilbert transform* will be central to our upcoming study in later chapters. It is related to the celebrated Fourier transform, which we will also use extensively. Before defining these transforms and looking at a few of their properties, we need the following definition.

Definition 3.1. *The space $L^p(\mathbb{R}^n)$ is set of all complex-valued functions on $\mathbb{R}^n$ that are p-th power integrable. That is, all functions $f\colon \mathbb{R}^n \to \mathbb{C}$ for which*

$$\int_{\mathbb{R}^n} |f|^p \, dx < \infty.$$

In general, the L^p spaces are defined in a measure theoretic framework (cf. [3, p. 409]), where the integral is to be understood as a Lebesgue integral. Such a theory ultimately becomes indispensable, but since it is not a requisite for deriving the desired results in this paper, we will not belabor our discussion with this generalization. For our purposes, the integral can be thought of as the traditional Riemann integral, and we will mostly be concerned with the case where $p = 1, 2$ and $n = 1, 2$.

There are several conventions for defining the Fourier transform, and little conformity in the literature. We have here chosen the definition convention from [3, p. 288].

Definition 3.2 (Fourier transform on L^1)**.** *Let $f \in L^1(\mathbb{R}^n)$. The Fourier transform of f, denoted by $\mathcal{F}[f]$ (and sometimes by $\widehat{f}$), is given by*

$$\mathcal{F}[f](y) = \widehat{f}(y) := \int_{\mathbb{R}^n} f(x) e^{-2\pi i x y} \, dx, \quad y \in \mathbb{R}^n,$$

where $xy = x_1y_1 + \cdots x_ny_n$.

Defining the Fourier transform in this way is preferred here, because the factor 2π is kept in the exponent and does not appear as a multiplicative factor outside the integrals, giving the upcoming inversion formula and convolution theorem a tidier look. Moving on, we have that if f, $\widehat{f} \in L^1(\mathbb{R}^n)$, then (cf. [3, p. 303])

$$f(x) = \mathcal{F}^{-1}[\widehat{f}](x) = \int_{\mathbb{R}^n} \widehat{f}(y) e^{2\pi i x y}\, dy, \tag{3.1}$$

which is occasionally referred to as the *Fourier inversion formula*. Due to linearity of integration, $\mathcal{F}$ and $\mathcal{F}^{-1}$ are both linear operators. One can also demonstrate other basic properties of the Fourier transform, e.g. how the Fourier transform works together with differentiation. We summarize some of these results below.

Proposition 3.1. *Let* f, $g \in L^1(\mathbb{R}^n)$, $h \in L^1(\mathbb{R})$. *Then*

(a) $\mathcal{F}[f * g](y) = \mathcal{F}[f](y) \cdot \mathcal{F}[g](y)$

(b) $\mathcal{F}\left[\frac{d^n}{dx^n}h\right](y) = (2\pi i y)^n \mathcal{F}[h](y)$

(c) $\mathcal{F}\left[\frac{1}{x^2+a^2}\right](y) = \frac{\pi}{a} e^{-2\pi a|y|}$, $a > 0$

Equation (a) is the convolution theorem. We recall the definition of a convolution as

$$(f * g)(x) = \int_{\mathbb{R}^n} f(x-y)g(y)\, dy = \int_{\mathbb{R}^n} f(y)g(x-y)\, dy,$$

where the final equality follows from a change of variables.

Proof. We omit the proofs of the fairly standard results (a) and (b). A more general proof of (b) involving partial derivatives can be found in [17, p. 33-34], where the domain of h need not be restricted to the real line[1]. The sought Fourier transform in (c) can be computed directly using contour integration. However, we have that

$$\begin{aligned}
\mathcal{F}^{-1}\left[\frac{\pi}{a}e^{-2\pi a|y|}\right](x) &= \int_{-\infty}^{\infty} \frac{\pi}{a} e^{-2\pi a|y|} e^{2\pi i x y}\, dy = \frac{\pi}{a}\int_{-\infty}^{0} e^{2\pi(a+ix)y}\, dy + \frac{\pi}{a}\int_{0}^{\infty} e^{2\pi(-a+ix)y}\, dy \\
&= \frac{\pi}{a} \lim_{R\to\infty} \left[\frac{1}{2\pi(a+ix)}\left(1 - e^{-2\pi(a+ix)R}\right) + \frac{1}{2\pi(-a+ix)}\left(e^{2\pi(-a+ix)R} - 1\right)\right] \\
&= \frac{1}{2a}\left[\frac{1}{a+ix} - \frac{1}{-a+ix}\right] = \frac{1}{x^2+a^2}.
\end{aligned}$$

Now apply the Fourier inversion formula (3.1) to get the desired result. □

[1] However, the function is assumed to belong to a space of rapidly decreasing functions; the Schwartz class S.

We now turn to the Hilbert transform, for which we restrict our attention to functions defined on $\mathbb{R}$.

Definition 3.3 (Hilbert transform on $\mathbb{R}$)**.** *Let $f \in L^1(\mathbb{R})$. The Hilbert transform of f, denoted by $\mathcal{H}[f]$, is defined as*

$$\mathcal{H}[f](x) := p.v.\frac{1}{\pi}\int_{\mathbb{R}} \frac{f(y)}{x-y}\,dy = p.v.\frac{1}{\pi}\int_{\mathbb{R}} \frac{f(x-y)}{y}\,dy = f * \frac{1}{\pi x},$$

where p.v. denotes the Cauchy principal value.

Recall that the Cauchy principal value is a way of coping with singularities in the interval of integration. Assigning a value to such an integral is achieved through a limiting process [12, p. 14]:

$$\text{p.v.}\int_a^b f(x)\,dx = \lim_{\varepsilon\to 0}\left(\int_a^{t-\varepsilon} f(x)\,dx + \int_{t+\varepsilon}^b f(x)\,dx\right),$$

where the function f has a singularity at $x = t$. We then proceed with a short lemma for use in a proof later on.

Lemma 3.1. *If $f(x) = c$, $c \in \mathbb{R}$, then $\mathcal{H}[f](x) = 0$.*

Proof. The calculation is straightforward from the definition:

$$\begin{aligned}\mathcal{H}[f](x) &:= \text{p.v.}\frac{1}{\pi}\int_{-\infty}^{\infty}\frac{c}{x-y}\,dy = \frac{c}{\pi}\lim_{R\to\infty}\lim_{\varepsilon\to 0}\left(\int_{-R}^{x-\varepsilon}\frac{1}{x-y}\,dy + \int_{x+\varepsilon}^{R}\frac{1}{x-y}\,dy\right)\\ &= \frac{c}{\pi}\lim_{R\to\infty}\lim_{\varepsilon\to 0}\log\left(\frac{x+R}{x-R}\right) = 0.\end{aligned}$$

□

Theorem 3.1 (Fourier and Hilbert transform)**.** *[12, p. 253] The Fourier and Hilbert transforms are related by*

$$\mathcal{F}\{\mathcal{H}[f]\}(\xi) = -i\,\text{sgn}(\xi)\mathcal{F}[f](\xi).$$

To close this section, we want to establish a final result regarding the Hilbert transform, which will be needed later in our derivation of the nonlinear evolution equations (see Chapters 4 and 5). We will state it here as a theorem, although it might not be general enough to deserve such a label. Its proof given here relies on several familiar results from complex analysis, which have been put in Appendix A to avoid what we would consider a lengthier digression.

Theorem 3.2. *Let $f(x) = e^{ikx}$. Then*

$$\mathcal{H}[f](x) = -i\,\text{sgn}(k)e^{ikx} \tag{3.2}$$

for any $k \in \mathbb{R}$.

Proof. By definition, we want to evaluate[2]

$$\mathcal{H}[f](x) = \frac{1}{\pi}\int_{-\infty}^{\infty}\frac{e^{ikt}}{x-t}dt.$$

Now, the singularity at $t = x$ poses a difficulty. To circumvent this issue, we can integrate along an indented path, as shown in Figure A.1.
For $k > 0$, let

$$F(z) = \frac{1}{\pi}\frac{1}{z_0 - z}e^{ikz},\ z = x + iy \in \mathbb{C},$$

and let C_R, C_ρ, L_1 and L_2 be as described in Definition A.1. Since $F(z)$ is holomorphic on and inside the contour $C = C_R \cup L_1 \cup C_\rho \cup L_2$, we have by the Cauchy-Goursat theorem (Theorem A.1) that

$$\int_C F(z)dz = 0,$$

which can be rewritten to give

$$\int_{L_1} F(z)dz + \int_{L_2} F(z)dz = -\int_{C_R} F(z)dz - \int_{C_\rho} F(z)dz.$$

In the limits $R \to \infty$ and $\rho \to 0$, the first integral on the right vanishes by Jordan's lemma[3], and the two integrals on the left formally become

$$\frac{1}{\pi}\int_{-\infty}^{\infty}\frac{1}{x_0 - x}e^{ikx}dx.$$

Thus

$$\frac{1}{\pi}\int_{-\infty}^{\infty}\frac{1}{x_0 - x}e^{ikx}dx = -\lim_{\substack{\rho\to 0\\ R\to\infty}}\int_{C_\rho} F(z)dz = i\pi\operatorname*{Res}_{z=z_0} F(z),$$

where the final equality follows from Theorem A.2. The residue of $F(z)$ can be evaluated using its Laurent series representation:

$$F(z) = -\frac{1}{\pi}e^{ikz_0}\frac{1}{z - z_0} - \frac{1}{\pi}ike^{ikz_0} + \frac{1}{2}\frac{1}{\pi}k^2e^{ikz_0}(z - z_0) + \cdots$$

from which we conclude that $\operatorname*{Res}_{z=z_0} F(z) = -\frac{1}{\pi}e^{ikz_0}$. Consequently,

$$\frac{1}{\pi}\int_{-\infty}^{\infty}\frac{1}{x_0 - x}e^{ikx}dx = -ie^{ikx_0},\ \text{for } k > 0.$$

For $k < 0$, the proof is similar, but in this case the paths C_R and C_ρ are in the lower half-plane. One will find that (cf. [13, pp. 12-13])

$$\frac{1}{\pi}\int_{-\infty}^{\infty}\frac{1}{x_0 - x}e^{ikx}dx = ie^{ikx_0}$$

[2] We have changed the integration variable y to t, to avoid confusion with the complex number $z = x+iy$.
[3] $f(z) = \frac{1}{\pi}\frac{1}{z_0 - z}$ in this application of Jordan's lemma.

For $k = 0$, $F(z)$ is a constant function, and by Lemma 3.1 the Hilbert transform of a constant function is zero. We finally conclude that

$$\frac{1}{\pi}\int_{-\infty}^{\infty}\frac{1}{x_0 - x}e^{ikx}dx = -i\,\mathrm{sgn}(k)e^{ikx_0}, \text{ for any } k \in \mathbb{R}.$$

which is the desired result after relabeling the symbols. This completes the proof. □

3.2 Solving the half-plane Neumann problem

Let $\mathbb{R}^2_+$ denote the upper half-plane in $\mathbb{R}^2$, with boundary $\partial\mathbb{R}^2_+$. That is,

$$\mathbb{R}^2_+ = \{(x, y) \in \mathbb{R}^2 : y > 0\}, \quad \partial\mathbb{R}^2_+ = \{(x, y) \in \mathbb{R}^2 : y = 0\}.$$

Here we will look at how one can use a Fourier transform method [8, pp. 182-190] to solve the upper half-plane Neumann problem

$$\begin{cases} \triangle u(x, y) = 0, & (x, y) \in \mathbb{R}^2_+, \\ u_y = g(x), & (x, y) \in \partial\mathbb{R}^2_+. \end{cases} \tag{3.3}$$

This boundary value problem will appear in our derivation of the nonlinear model equations in Chapters 4 and 5, and its solution is given here for the sake of completing the discussion. To solve problem (3.3), we begin by taking the Fourier transform in the variable x on both sides of the Laplace equation and using that $\widehat{\partial_x u}(\xi) = 2\pi i\xi\widehat{u}(\xi)$ (cf. Proposition 3.1), resulting in

$$\mathcal{F}\left[u_{xx} + u_{yy}\right](\xi, y) = -4\pi^2\,\widehat{u}(\xi, y) + \widehat{u}_{yy}(\xi, y) = 0,$$

or

$$\widehat{u}_{yy}(\xi, y) = 4\pi^2\,\widehat{u}(\xi, y).$$

For fixed ξ, this is an ODE in the variable y, with general solution

$$\widehat{u}(\xi, y) = A(\xi)e^{-2\pi|\xi|y} + B(\xi)e^{2\pi|\xi|y}.$$

We require $\widehat{u}$ to be bounded as $y \to \infty$, therefore $B(\xi) \equiv 0$. Furthermore, because $u_y(x, 0) = g(x)$, we have that

$$\widehat{u}_y(\xi, 0) = \widehat{g}(\xi) = -2\pi A(\xi)|\xi|,$$

which gives

$$\widehat{u}(\xi, y) = \frac{-\widehat{g}(\xi)}{2\pi|\xi|}e^{-2\pi|\xi|y} = -i\,\mathrm{sgn}(\xi)\frac{\widehat{g}(\xi)e^{-2\pi|\xi|y}}{2\pi i\xi}.$$

So, according to Theorem 3.1

$$u(x, y) = \mathcal{H}\left\{\mathcal{F}^{-1}\left[\frac{\widehat{g}(\xi)e^{-2\pi|\xi|y}}{2\pi i\xi}\right](x, y)\right\}, \tag{3.4}$$

where the Hilbert transform $\mathcal{H}$ is taken in the variable x. For the expression inside the curly braces in eq. (3.4), we apply the convolution theorem:

$$u(x,y) = \mathcal{H}\left\{\mathcal{F}^{-1}\left[\frac{\widehat{g}(\xi)}{2\pi i\xi}\right] * \mathcal{F}^{-1}\left[e^{-2\pi|\xi|y}\right](x,y)\right\}.$$

From eq. (c) in Proposition 3.1, we now get

$$u(x,y) = \mathcal{H}\left\{\mathcal{F}^{-1}\left[\frac{\widehat{g}(\xi)}{2\pi i\xi}\right] * \left[\frac{1}{\pi}\frac{y}{x^2+y^2}\right](x,y)\right\}. \tag{3.5}$$

Using that $\mathcal{F}\left[\partial_x^{-1}h\right](\xi) = \frac{\widehat{h}(\xi)}{2\pi i\xi}$, where the notation ∂_x^{-1} signifies an inverse differentiation operator[4], eq. (3.5) becomes

$$u(x,y) = \mathcal{H}\left\{\left[\partial_x^{-1}g\right] * \left[\frac{1}{\pi}\frac{y}{x^2+y^2}\right](x,y)\right\} = \mathcal{H}\left\{\partial_x^{-1}P_y[g](x,y)\right\}, \tag{3.6}$$

where we have applied the notation

$$P_y[g](x,y) = \int_{-\infty}^{\infty}\frac{y}{(x-s)^2+y^2}g(s)ds$$

for the Poisson integral operator (cf. [12, pp. 375]). Now,

$$u(x,0) = \mathcal{H}\left\{\partial_x^{-1}P_0[g]\right\} = \mathcal{H}\left\{\partial_x^{-1}g\right\}.$$

In the special case when the boundary function $g(x)$ is given as a derivative, say $g(x) = G'(x)$, we have that

$$u(x,y) = \mathcal{H}\left\{P_y[G](x,y)\right\}, \quad u(x,0) = \mathcal{H}\left\{G\right\}. \tag{3.7}$$

This can be realized from eq. 3.5 by noting that

$$\mathcal{F}^{-1}\left\{\frac{\widehat{\partial_x G}(\xi)}{2\pi i\xi}\right\} = \mathcal{F}^{-1}\left\{\frac{2\pi i\xi\widehat{G}(\xi)}{2\pi i\xi}\right\} = G(x),$$

Alternatively, as pointed out earlier, one can view ∂_x and ∂_x^{-1} as inverse operators in eq. (3.6).

3.3 Discrete cosine transform

A discrete cosine transform (DCT) of a sequence of real numbers can be derived by applying the discrete Fourier transform (DFT) to an even extension of that sequence. Different even extensions of the sequence are possible, yielding different definitions of the DCT [15, p. 28].

[4]The usage of this notation in later developments are in formal arguments. It can also be found in [10].

We will here choose an extension leading to a DCT that conforms with the developments in [7] and [11], where the spectral collocation scheme is discussed (see Chapter 5), and where the DCT is needed to compute the Fourier cosine coefficients. The subsequent derivation of the DCT is based on that given in [15, pp. 27-29], but we will slightly modify the approach to arrive at a final expression not containing complex exponential functions as in the cited literature.

Let $x(n)$, $n = 0, 1, ..., N-1$, be a sequence of real numbers, and let $y(n)$ be a $2N$-point even extension of $x(n)$. That is,

$$y(n) = \begin{cases} x(n), & n = 0, ..., N-1, \\ x(2N-1-n), & n = N, ..., 2N-1. \end{cases} \tag{3.8}$$

The derivation of the DCT in [15] is based on (3.8). We will, with a similar approach, derive a more "direct" expression.

Let $z(n)$ be the $4N$-point sequence which is zero at even indices, and have the values of $y(n)$ (in order) at odd indices. More precisely, let

$$z(n) = \begin{cases} y(\frac{n-1}{2}), & n = 2m+1, \\ 0, & n = 2m, \end{cases} \qquad m = 0, 1..., 2N-1. \tag{3.9}$$

By definition, the DFT of $z(n)$ is given by

$$Z(k) = \sum_{n=0}^{4N-1} z(n) w^{nk}, \quad w = e^{\frac{-i\pi}{2N}}. \tag{3.10}$$

Applying the DFT to eq. (3.9), we get

$$Z(k) = \sum_{m=0}^{2N-1} z(2m+1) w^{(2m+1)k} = \sum_{m=0}^{2N-1} y(m) w^{(2m+1)k},$$

where the first equality is due to fact that $z(n)$ vanishes at even indices. We may further use the definition of $y(n)$ to write

$$\begin{aligned} Z(k) &= \sum_{m=0}^{N-1} x(m) w^{(2m+1)k} + \sum_{m=N}^{2N-1} x(2N-1-m) w^{(2m+1)k} \\ &= \sum_{m=0}^{N-1} x(m) \left[w^{(2m+1)k} + w^{(-2m-1)k} \right] = 2 \sum_{m=0}^{N-1} x(m) \cos\left(\frac{\pi}{2N} (2m+1) k \right), \end{aligned} \tag{3.11}$$

where the second equality follows from a change of summation index and because $w^{4Nk} = 1$ for integer k, and the last equality is due to Euler's formula. From eq. (3.11) we define the DCT of the sequence $x(n)$.

Definition 3.4 (Discrete cosine transform)**.** *Let $x(n)$ be an N-point sequence of real numbers. The discrete cosine transform (DCT) of $x(n)$ is given by*

$$C(k) = \sum_{n=0}^{N-1} x(n) \cos\left(\frac{\pi}{2N}(2n+1)k\right), \quad k = 0, ..., N-1. \tag{3.12}$$

As pointed out, the discrete cosine transform will come up in Chapter 5 when we discuss the numerical method and its spectral collocation scheme.

Chapter 4

Nonlinear model equations

This chapter presents a derivation of some two-dimensional nonlinear model equations of waves primarily propagating in the x direction, with a weak transverse variation. Later we will restrict our model to waves propagating in one direction; the direction of increasing values of x. We close the chapter with a connection between the obtained model equation and the dispersion relation derived in Chapter 2. Despite not having the numerical machinery at our disposal to analyze the two-dimensional equations arising, we present the general derivation here partly to pave the way for future developments. Numerical methods employed on a one-dimensional model is given in the next chapter.

4.1 Preliminaries

We begin by recalling the field equations and boundary conditions from Chapter 2. There we argued that the velocity potentials for each fluid layer must satisfy a Laplace equation. The velocity potentials ϕ, ψ and the interface deflection η are related and constrained under kinematic and dynamic boundary conditions. To summarize our findings from earlier work, we will like to study the problems

$$\triangle\phi = 0, \quad -h_0 < z < \eta, \tag{4.1}$$

$$\triangle\psi = 0, \quad \eta < z < \infty, \tag{4.2}$$

subject to the boundary conditions

$$\left.\begin{aligned} -(U_1+\phi_x)\eta_x - \phi_y\eta_y + \phi_z &= \eta_t, && (4.3)\\ -(U_2+\psi_x)\eta_x - \psi_y\eta_y + \psi_z &= \eta_t, && (4.4)\\ \rho_1\left(\phi_t + U_1\phi_x + \tfrac{1}{2}|\nabla\phi|^2 + g\eta\right) - \rho_2\left(\psi_t + U_2\psi_x + \tfrac{1}{2}|\nabla\psi|^2 + g\eta\right) &= \tau\eta_{xx}, && (4.5)\end{aligned}\right\}$$

which are evaluated at the interface $z = \eta$.

Nondimensionalization

It is advantageous to recast the field equations (4.1)-(4.2) and boundary conditions (4.3)-(4.5) in dimensionless form. Besides aiding the subsequent computations, a proper nondimensional formulation of the equations helps reflecting the problem geometry and bring to light the relative importance of terms by the size of appearing coefficients. To this end, we apply the following scalings, where original variables appear with a prime [1, pp. 105-106], [10]:

$$\begin{aligned} z' &= \lambda Z, \quad \eta' < z' < \infty, \\ z' &= h_0 z, \quad -h_0 < z' < \eta'. \end{aligned}$$

As can be seen, the variables are normalized differently in each layer, reflecting the asymmetry in length scales in the vertical direction. For the remaining variables, we let

$$x' = \lambda x, \quad y' = \Lambda y, \quad t' = \frac{\lambda}{c_0 v_0} t,$$

and

$$\eta' = a\eta, \quad \phi' = \frac{ag\lambda v_0}{c_0}\phi, \quad \psi' = \frac{ag\lambda v_0}{c_0}\psi.$$

In these latter expressions, $c_0 = \sqrt{gh_0}$ is the limiting long-wave speed, and $v_0^2 = 1 - \frac{\rho_2}{\rho_1}$. It is helpful to introduce the dimensionless parameters

$$\varepsilon = \frac{h_0}{\lambda}, \quad \delta = \frac{\lambda}{\Lambda}, \quad \sigma = \frac{a}{h_0}, \quad \mu = \frac{\tau}{(\rho_1 - \rho_2) g \lambda^2}. \tag{4.6}$$

Throughout this study we will assume that the typical longitudinal wavelength λ is large compared with the undisturbed depth h_0, that λ is small compared to Λ, and that the wave amplitude a is small compared to the depth h_0. This will imply that the dimensionless quantities ε, δ^2, σ and μ are small, and they are further assumed to be of the same order.

Applying these scalings and the chain rule of differentiation, the kinematic conditions (4.3)-(4.4) are readily converted to

$$\begin{aligned} \frac{ac_0v_0}{\lambda}\eta_t + \frac{a}{\lambda}\left(U_1 + \frac{agv_0}{c_0}\phi_x\right)\eta_x + \frac{a^2g\lambda v_0}{c_0\Lambda^2}\phi_y\eta_y &= \frac{ag\lambda v_0}{c_0 h_0}\phi_z, \quad z = \sigma\eta, \\ \frac{ac_0v_0}{\lambda}\eta_t + \frac{a}{\lambda}\left(U_2 + \frac{agv_0}{c_0}\psi_x\right)\eta_x + \frac{a^2g\lambda v_0}{c_0\Lambda^2}\psi_y\eta_y &= \frac{agv_0}{c_0}\psi_Z, \quad Z = \varepsilon\sigma\eta, \end{aligned}$$

or, upon diving out common factors and applying the expressions in (4.6),

$$\eta_t + \left(\frac{U_1}{c_0v_0} + \sigma\phi_x\right)\eta_x + \sigma\delta^2\phi_y\eta_y = \frac{1}{\varepsilon^2}\phi_z, \quad z = \sigma\eta, \tag{4.7}$$

$$\eta_t + \left(\frac{U_2}{c_0v_0} + \sigma\psi_x\right)\eta_x + \sigma\delta^2\psi_y\eta_y = \frac{1}{\varepsilon}\psi_Z, \quad Z = \varepsilon\sigma\eta. \tag{4.8}$$

In a similar manner, the dynamic condition (4.5) is converted to

$$\eta + \phi_t + \frac{U_1}{c_0 v_0}\phi_x + \frac{1}{2}\sigma\left(\phi_x^2 + \delta^2\phi_y^2 + \frac{1}{\varepsilon^2}\phi_z^2\right) - \frac{\rho_2}{\rho_1}\left[\psi_t + \frac{U_2}{c_0 v_0}\psi_x + \frac{1}{2}\sigma\left(\psi_x^2 + \delta^2\psi_y^2 + \psi_Z^2\right)\right]$$

$$= \mu\eta_{xx}, \quad z = \sigma\eta, \quad Z = \varepsilon\sigma\eta. \tag{4.9}$$

Subtracting (4.7) from (4.8) yields

$$\frac{U_2 - U_1}{c_0 v_0}\eta_x + \sigma\left(\psi_x - \phi_x\right)\eta_x + \sigma\delta^2\left(\psi_y - \phi_y\right)\eta_y = \frac{1}{\varepsilon}\psi_Z - \frac{1}{\varepsilon^2}\phi_z,$$

or

$$\psi_Z = \frac{1}{\varepsilon}\phi_z + \varepsilon\frac{U_2 - U_1}{c_0 v_0}\eta_x + \varepsilon\sigma\left(\psi_x - \phi_x\right)\eta_x + \varepsilon\delta^2\sigma\left(\psi_y - \phi_y\right)\eta_y,\ z = \sigma\eta,\ Z = \varepsilon\sigma\eta, \tag{4.10}$$

after multiplying through by ε and rearranging. Lastly, we need the normalized version of the Laplace equation (4.1),

$$\triangle'\phi' = \phi'_{x'x'} + \phi'_{y'y'} + \phi'_{z'z'} = 0,$$

which becomes

$$\triangle\phi = \varepsilon^2\phi_{xx} + \varepsilon^2\delta^2\phi_{yy} + \phi_{zz} = 0, \quad -1 < z < \sigma\eta, \tag{4.11}$$

where $\triangle = \varepsilon^2\partial_{xx} + \varepsilon^2\delta^2\partial_{yy} + \partial_{zz}$ is the normalized Laplace operator.

4.2 System of nonlinear equations

Formal asymptotic expansion

Similar to the treatment of shallow water surface gravity waves in [18, pp. 464-466], we wish to solve (4.11) by expanding the velocity potential in a formal series about $z = -1$:

$$\phi = \sum_{n=0}^{\infty}(z+1)^n f_n(x, y, t).$$

Substituting this expression into the normalized Laplace equation (4.11) yields

$$\left(\tilde{\triangle}f_0 + 2\cdot 1 f_2\right) + \left(\tilde{\triangle}f_1 + 3\cdot 2 f_3\right)(z+1) + \left(\tilde{\triangle}f_2 + 4\cdot 3 f_4\right)(z+1)^2 + \cdots = 0,$$

where $\tilde{\triangle} = \varepsilon^2\partial_{xx} + \varepsilon^2\delta^2\partial_{yy}$. We thereby get

$$\begin{aligned}
f_2 &= -\frac{1}{2!}\tilde{\triangle}f_0, \\
f_3 &= -\frac{1}{3\cdot 2}\tilde{\triangle}f_1 = -\frac{1}{3!}\tilde{\triangle}f_1, \\
f_4 &= -\frac{1}{4\cdot 3}\tilde{\triangle}f_2 = \frac{1}{4!}\tilde{\triangle}^2 f_0, \\
f_5 &= -\frac{1}{5\cdot 4}\tilde{\triangle}f_3 = \frac{1}{5!}\tilde{\triangle}^2 f_1, \\
&\vdots
\end{aligned}$$

Applying the fluid bottom boundary condition $\phi_z(z=-1)=0$ (see eq. (2.5)), we obtain

$$\phi_z(x,y,-1,t)=\sum_{n=1}^{\infty} n(z+1)^{n-1} f_n(x,y,t)\Big|_{z=-1} = f_1(x,y,t)=0.$$

From the expressions we found above:

$$f_{2m}=\frac{(-1)^m}{(2m)!}\tilde{\triangle}^{2m} f_0(x,y,t),$$
$$f_{2m+1}=0, \quad m=0,1,2,\ldots,$$

and we arrive at

$$\phi(x,y,z,t)=\sum_{m=0}^{\infty}\frac{(-1)^m}{(2m)!}(z+1)^{2m}\tilde{\triangle}^{2m} f_0(x,y,t).$$

Relabeling f_0 to f, and writing out the first few terms of the expansion gives

$$\phi = f-\frac{\varepsilon^2}{2}\left(f_{xx}+\delta^2 f_{yy}\right)(z+1)^2+\frac{\varepsilon^4}{24}\left(f_{xxxx}+\delta^2 f_{xxyy}+\delta^4 f_{yyyy}\right)(z+1)^4+\cdots.$$

So

$$\phi_z=-\varepsilon^2\left(f_{xx}+\delta^2 f_{yy}\right)(z+1)+\mathcal{O}(\varepsilon^4),$$

which when substituted into equation (4.10) gives

$$\psi_Z=-\varepsilon\left(f_{xx}+\delta^2 f_{yy}\right)(1+\sigma\eta)+\frac{U_2-U_1}{c_0 v_0}\eta_x+\mathcal{O}(\varepsilon^2,\varepsilon\sigma), \quad Z=\varepsilon\sigma\eta. \tag{4.12}$$

Elliptic PDE and its solution

The following derivation is based on that given in [10]. The second Laplace equation (4.2) and the merged boundary condition (4.12) now yield the following upper half-plane Neumann problem:

$$\begin{cases}\triangle\psi=0, \quad Z>\varepsilon\sigma\eta,\\ \psi_Z=-\varepsilon(1+\sigma\eta)(f_{xx}+\delta^2 f_{yy})+\varepsilon\frac{U_2-U_1}{c_0 v_0}\eta_x+\mathcal{O}(\varepsilon^2,\varepsilon\sigma), \quad Z=\varepsilon\sigma\eta,\end{cases} \tag{4.13}$$

where $\triangle=\partial_{xx}+\delta^2\partial_{yy}+\partial_{ZZ}$. The problem (4.13) may be shifted to the more tractable half-plane problem

$$\begin{cases}\triangle\psi=0, \quad Z>0,\\ \psi_Z=-\varepsilon(f_{xx}+\delta^2 f_{yy})+\varepsilon\frac{U_2-U_1}{c_0 v_0}\eta_x, \quad Z=0,\end{cases} \tag{4.14}$$

achieved by expanding the boundary function ψ_Z in a Taylor series about $Z=0$, and dropping higher order terms. This type of Neumann problem was discussed in Chapter 3.

Applying that theory here, we take the Fourier transform in x and y on both sides of the normalized Laplace equation for ψ:

$$\mathcal{F}_{x,y}\left[\psi_{xx}+\delta^2\psi_{yy}+\psi_{ZZ}\right](\xi,\nu,Z)=-\xi^2\widehat{\psi}-\delta^2\nu^2\widehat{\psi}+\widehat{\psi}_{ZZ}=0,$$

which for fixed ξ and ν is an ODE in Z. The (bounded) solution is

$$\widehat{\psi}=C(\xi,\nu)\exp\left\{-\sqrt{\xi^2+\delta^2\nu^2}Z\right\}=C(\xi,\nu)\exp\left\{-|\xi|\sqrt{1+\delta^2\nu^2/\xi^2}Z\right\}. \tag{4.15}$$

In (4.15), we have already neglected the unbounded part of the general solution, corresponding to a positive exponent. From the boundary condition in (4.14), we have

$$\widehat{\psi}_Z\Big|_{Z=0}=-C(\xi,\nu)|\xi|\sqrt{1+\delta^2\nu^2/\xi^2}=-\varepsilon\left(f_{xx}+\delta^2 f_{yy}\right)+\varepsilon\frac{U_2-U_1}{c_0v_0}\eta_x,$$

giving

$$\begin{aligned}C(\xi,\nu)&=\frac{1}{|\xi|\sqrt{1+\theta^2}}\,\varepsilon\left(\widehat{f}_{xx}+\delta^2\widehat{f}_{yy}+\frac{U_1-U_2}{c_0v_0}\widehat{\eta}_x\right)\\&=\frac{1}{|\xi|}\,\varepsilon\left(1-\frac{1}{2}\theta^2+\frac{3}{8}\theta^4+\mathcal{O}\left(\theta^5\right)\right)\left(\widehat{f}_{xx}+\delta^2\widehat{f}_{yy}+\frac{U_1-U_2}{c_0v_0}\widehat{\eta}_x\right),\quad\theta=\frac{\delta\nu}{\xi},\end{aligned}$$

where we have expanded the reciprocal square root in a Taylor series about $\theta=0$. Neglecting higher order terms, we obtain

$$\begin{aligned}C(\xi,\nu)&=\frac{1}{|\xi|}\varepsilon\left(\widehat{f}_{xx}+\frac{U_1-U_2}{c_0v_0}\widehat{\eta}_x\right)=\frac{1}{|\xi|}\varepsilon\left(i\xi\widehat{f}_x+i\xi\frac{U_1-U_2}{c_0v_0}\widehat{\eta}\right)\\&=i\,\mathrm{sgn}(\xi)\varepsilon\left(\widehat{f}_x+\frac{U_1-U_2}{c_0v_0}\widehat{\eta}\right)\end{aligned}$$

and thus

$$\widehat{\psi}=i\,\mathrm{sgn}(\xi)\varepsilon\left(\widehat{f}_x+\frac{U_1-U_2}{c_0v_0}\widehat{\eta}\right)\exp\left\{-|\xi|\sqrt{1+\theta^2}Z\right\}. \tag{4.16}$$

Similarly to the previous treatment, the exponential function may be expanded in powers of θ:

$$\begin{aligned}\exp\left\{-|\xi|\sqrt{1+\theta^2}Z\right\}&=\exp\left\{-|\xi|Z\right\}\exp\left\{|\xi|\left(1-\sqrt{1+\theta^2}\right)Z\right\}\\&=\exp\left\{-|\xi|Z\right\}\left(1-\frac{1}{2}|\xi|Z\theta^2+\mathcal{O}\left(\theta^3\right)\right).\end{aligned}$$

Substitution into eq. (4.16) and disregarding higher order terms in ε and δ^2, gives

$$\widehat{\psi}(\xi,\nu,Z,t)=-i\,\mathrm{sgn}(\xi)\varepsilon\left(-\widehat{f}_x-\frac{U_1-U_2}{c_0v_0}\widehat{\eta}\right)\exp\left\{-|\xi|Z\right\}, \tag{4.17}$$

where we have added a minus sign in front of the expression for convenience regarding what follows. Applying Theorem 3.1, we get

$$\psi(x,y,Z,t) = \mathcal{H}\left\{\left[-\varepsilon f_x - \varepsilon\frac{U_1-U_2}{c_0v_0}\eta\right] * \left[\mathcal{F}_\xi^{-1}\left(e^{|\xi|Z}\right)\right]\right\}$$
$$= \varepsilon\mathcal{H}\left\{P_Z\left[\frac{U_2-U_1}{c_0v_0}\eta - f_x\right]\right\},$$

where the Hilbert transform $\mathcal{H}$ is taken in the variable x. Recall that P_Z is a Poisson integral operator for the upper half-plane (see Chapter 3). We thereby get,

$$\psi(x,y,0,t) = \varepsilon\mathcal{H}\left[\frac{U_2-U_1}{c_0v_0}\eta - f_x\right].$$

Consequently, to first order, we have

$$\phi_t = f_t, \quad \phi_x = f_x, \quad \phi_y = f_y, \quad \psi_t = \varepsilon\mathcal{H}\left[\frac{U_2-U_1}{c_0v_0}\eta_t - f_{xt}\right],$$
$$\psi_x = \varepsilon\mathcal{H}\left[\frac{U_2-U_1}{c_0v_0}\eta_x - f_{xx}\right], \quad \psi_y = \varepsilon\mathcal{H}\left[\frac{U_2-U_1}{c_0v_0}\eta_y - f_{xy}\right].$$

In addition, to higher order[1],

$$\phi_z = -\varepsilon^2(f_{xx}+\delta^2 f_{yy})(1+\sigma\eta), \quad \psi_Z = -\varepsilon(1+\sigma\eta)\left(f_{xx}+\delta^2 f_{yy}\right) + \frac{U_2-U_1}{c_0v_0}\eta_x.$$

Substitution of these expressions into the normalized dynamic condition (4.9) gives

$$\eta + f_t + \frac{U_1}{c_0v_0}f_x + \frac{1}{2}\sigma f_x^2 \tag{4.18}$$
$$- \varepsilon\frac{\rho_2}{\rho_1}\mathcal{H}\left[\frac{U_2(U_2-U_1)}{c_0^2v_0^2}\eta_x + \frac{U_2-U_1}{c_0v_0}\eta_t - \frac{U_2}{c_0v_0}f_{xx} - f_{xt}\right] - \mu\eta_{xx} = \mathcal{O}(\varepsilon^2\sigma, \sigma^2, \sigma\delta^2).$$

We proceed by differentiating eq. (4.18) with respect to x, writing $w = f_x$ and neglecting terms of higher order:

$$\eta_x + w_t + \frac{U_1}{c_0v_0}w_x + \sigma w w_x \tag{4.19}$$
$$- \varepsilon\frac{\rho_2}{\rho_1}\mathcal{H}\left[\frac{U_2(U_2-U_1)}{c_0^2v_0^2}\eta_{xx} + \frac{U_2-U_1}{c_0v_0}\eta_{xt} - \frac{U_2}{c_0v_0}w_{xx} - w_{xt}\right] - \mu\eta_{xxx} = 0.$$

From eq. (4.19) it is clear that

$$\eta_x + w_t + \frac{U_1}{c_0v_0}w_x = \mathcal{O}(\varepsilon,\sigma,\mu). \tag{4.20}$$

[1]It will be clear later why we must retain these terms to higher order.

Under the assumption that differentiation and the application of the Hilbert transform does not alter this order relation (cf. [10, p. 172]), we get

$$\mathcal{H}w_{xt} = -\mathcal{H}\eta_{xx} - \frac{U_1}{c_0 v_0}\mathcal{H}w_{xx} + \mathcal{O}(\varepsilon, \sigma, \mu). \tag{4.21}$$

Furthermore, from the kinematic condition (4.7),

$$\eta_t + \left(\frac{U_1}{c_0 v_0} + \sigma f_x\right)\eta_x + \delta^2 \sigma f_y \eta_y = -\frac{1}{\varepsilon^2}\varepsilon^2 \left(f_{xx} + \delta^2 f_{yy}\right)(1 + \sigma\eta).$$

This gives

$$\eta_t + \frac{U_1}{c_0 v_0}\eta_x + w_x = \mathcal{O}(\sigma, \delta^2), \tag{4.22}$$

and under the same assumptions leading to eq. (4.21),

$$\mathcal{H}\eta_{xt} = -\frac{U_1}{c_0 v_0}\mathcal{H}\eta_{xx} - \mathcal{H}w_{xx} + \mathcal{O}(\sigma, \delta^2). \tag{4.23}$$

Upon substituting eqs. (4.21) and (4.23) into eq. (4.19) and neglecting higher order terms, we obtain the first model equation for our nonlinear system:

$$\begin{aligned} &\eta_x + w_t + \frac{U_1}{c_0 v_0} w_x + \sigma w w_x \\ &\quad - \varepsilon \frac{\rho_2}{\rho_1}\mathcal{H}\left[2\frac{U_1 - U_2}{c_0 v_0} w_{xx} + \frac{(U_1 - U_2)^2}{c_0^2 v_0^2}\eta_{xx} + \eta_{xx}\right] - \mu\eta_{xxx} = 0. \end{aligned} \tag{4.24}$$

The second model equation in our system is eq. (4.7) rewritten with the obtained expressions for ϕ and its derivatives (the notation ∂_x^{-1} is explained in Chapter 3):

$$\eta_t + \frac{U_1}{c_0 v_0}\eta_x + w_x + \sigma\left(w\eta\right)_x + \delta^2\left(\partial_x^{-1} w\right)_{yy} = 0. \tag{4.25}$$

Equations (4.24) and (4.25) constitute our system of nonlinear evolution equations.

4.3 Wave propagation in one direction

We now focus our attention on waves propagating primarily in the positive x direction. As we will see, the system consisting of eqs. (4.24) and (4.25) reduces to a single model equation (cf. [10, p. 173]). As in the literature just cited, we wish to obtain a model equation correct to first order in the parameters ε, σ, μ and δ^2 (recall that they are all assumed to be of the same order). Therefore, we employ the ansatz

$$w = \eta + \varepsilon A + \sigma B + \mu C + \delta^2 D, \tag{4.26}$$

where A, B, C and D are functions of η and its derivatives. Substitution of eq. (4.26) into eq. (4.24), again after neglecting higher order terms, yields

$$\eta_t + \left(1 + \frac{U_1}{c_0 v_0}\right)\eta_x + \varepsilon\left[A_t + \frac{U_1}{c_0 v_0}A_x - \frac{\rho_2}{\rho_1}\left(\frac{U_2 - U_1}{c_0 v_0} - 1\right)^2 \mathcal{H}\eta_{xx}\right] + \sigma\left[B_t + \frac{U_1}{c_0 v_0}B_x + \eta\eta_x\right]$$
$$+\mu\left[C_t + \frac{U_1}{c_0 v_0}C_x - \eta_{xxx}\right] + \delta^2\left[D_t + \frac{U_1}{c_0 v_0}D_x\right] = 0. \tag{4.27}$$

Similarly, eq. (4.25) becomes

$$\eta_t + \left(1 + \frac{U_1}{c_0 v_0}\right)\eta_x + \varepsilon\left[A_x\right] + \sigma\left[B_x + 2\eta\eta_x\right] + \mu\left[C_x\right] + \delta^2\left[D_x + \partial_x^{-1}\eta_{yy}\right] = 0. \tag{4.28}$$

Since w is a function of η and its derivatives, and because

$$\eta_t = -\left(1 + \frac{U_1}{c_0 v_0}\right)\eta_x + \mathcal{O}(\varepsilon, \sigma, \mu, \delta^2),$$

we may replace A_t by $-A_x$ in (4.27), and similarly for B, C and D. This substitution is correct to second order (cf. [10, p. 173] and [18, p. 466]). Now, for eqs. (4.27) and (4.28) to be consistent with each other, we require that

$$\begin{aligned}
A_x &= \left(\frac{U_1}{c_0 v_0} - 1\right)A_x - \frac{\rho_2}{\rho_1}\left(\frac{U_2 - U_1}{c_0 v_0} - 1\right)^2 \mathcal{H}\eta_{xx},\\
B_x + 2\eta\eta_x &= \left(\frac{U_1}{c_0 v_0} - 1\right)B_x + \eta\eta_x,\\
C_x &= \left(\frac{U_1}{c_0 v_0} - 1\right)C_x - \eta_{xxx},\\
D_x + \partial_x^{-1}\eta_{yy} &= \left(\frac{U_1}{c_0 v_0} - 1\right)D_x.
\end{aligned}$$

After rearranging and integrating with respect to x, we obtain

$$\begin{aligned}
&A = -\frac{\rho_2}{\rho_1}\left(2 - \frac{U_1}{c_0 v_0}\right)^{-1}\left(\frac{U_2 - U_1}{c_0 v_0} - 1\right)^2 \mathcal{H}\eta_x, \quad B = -\frac{1}{2}\left(2 - \frac{U_1}{c_0 v_0}\right)^{-1}\eta^2,\\
&C = -\left(2 - \frac{U_1}{c_0 v_0}\right)^{-1}\eta_{xx}, \quad D = -\left(2 - \frac{U_1}{c_0 v_0}\right)^{-1}\partial_x^{-1}\partial_x^{-1}\eta_{yy}.
\end{aligned}$$

Recalling eq. (4.26) and substituting this into the second model equation (4.25), we finally obtain the unidirectional model equation

$$\eta_t + \left(1 + \frac{U_1}{c_0 v_0}\right)\eta_x + \sigma\left[2 - \left(2 - \frac{U_1}{c_0 v_0}\right)^{-1}\right]\eta\eta_x - \varepsilon\left(2 - \frac{U_1}{c_0 v_0}\right)^{-1}\left(\frac{U_2 - U_1}{c_0 v_0} - 1\right)^2 \frac{\rho_2}{\rho_1}\mathcal{H}\eta_{xx}$$
$$-\mu\left(2 - \frac{U_1}{c_0 v_0}\right)^{-1}\eta_{xxx} + \delta^2\left[1 - \left(2 - \frac{U_1}{c_0 v_0}\right)^{-1}\right]\partial_x^{-1}\eta_{yy} = 0. \tag{4.29}$$

Special cases

In the case when there is no imposed shear flow, $U_1 = U_2 = 0$, eq. (4.29) reduces to

$$\eta_t + \eta_x + \frac{3}{2}\sigma\eta\eta_x - \frac{1}{2}\mu\eta_{xxx} + \frac{1}{2}\delta^2\partial_x^{-1}\eta_{yy} = 0. \tag{4.30}$$

Upon differentiating both sides of (4.30) with respect to x, we obtain a form of the Kadomtsev-Petviashvili (KP) equation

$$\left(\eta_t + \eta_x + \frac{3}{2}\sigma\eta\eta_x - \frac{1}{2}\mu\eta_{xxx}\right)_x + \frac{1}{2}\delta^2\eta_{yy} = 0, \tag{4.31}$$

which can be seen as a two-dimensional generalization of the KdV equation [5, p. 38].

If we on the other hand restrict our model (4.29) to one dimension, i.e. neglecting the y derivative term, and assume only $U_1 = 0$, we get (writing $U = U_2$)

$$\eta_t + \eta_x + \frac{3}{2}\sigma\eta\eta_x - \varepsilon\frac{1}{2}\frac{\rho_2}{\rho_1}\left(\frac{U}{c_0 v_0} - 1\right)^2 \mathcal{H}\eta_{xx} - \mu\frac{1}{2}\eta_{xxx} = 0, \tag{4.32}$$

which is the model equation we will study numerically in Chapter 5 after applying an additional normalization.

4.4 Linearized model equation and dispersion relation

The model system consisting of eqs. (4.24) and (4.25) may be linearized to obtain a single linear evolution equation. First, let us put the system back in dimensional form:

$$g v_0^2\eta_x + w_t + U_1 w_x + w w_x - \frac{\rho_2}{\rho_1}\mathcal{H}\left[2(U_1 - U_2)h_0 w_{xx} + (U_1 - U_2)^2\eta_{xx} + c_0^2 v_0^2\eta_{xx}\right] - \frac{\tau}{\rho_1}\eta_{xxx} = 0, \tag{4.33}$$

$$\eta_t + U_1\eta_x + h_0 w_x + (w\eta)_x = 0. \tag{4.34}$$

Eq. (4.34) may be rewritten like

$$w_x = -\frac{1}{h_0}(\eta_t + U_1\eta_x) + \text{quadratic terms},$$

where by quadratic terms we mean quadratic terms in η, w and their derivatives. Upon neglecting these we obtain

$$w_{xt} = -\frac{1}{h_0}(\eta_{tt} + U_1\eta_{xt}),\ w_{xx} = -\frac{1}{h_0}(\eta_{xt} + U_1\eta_{xx}),\ w_{xxx} = -\frac{1}{h_0}(\eta_{xxt} + U_1\eta_{xxx}).$$

Substituting these expressions into eq. (4.33), we arrive at the linearized model equation

$$\eta_{tt} + (U_1^2 - c_0^2 v_0^2)\eta_{xx} + 2U_1\eta_{xt} + h_0\frac{\rho_2}{\rho_1}\mathcal{H}\left[2(U_2 - U_1)\eta_{xxt} + (U_2^2 - U_1^2 + c_0^2 v_0^2)\eta_{xxx}\right] - \frac{h_0\tau}{\rho_1}\eta_{xxxx} = 0. \tag{4.35}$$

Now, if we assume simple sinusoidal waveforms (cf. Chapter 2)

$$\eta = e^{ik(x-ct)}, \tag{4.36}$$

eq. (4.35) gives the dispersion relation

$$\begin{aligned}\omega^2 + 2\left\{h_0\mathcal{R}(U_1-U_2)k|k| - U_1 k\right\}\omega \\ + \left\{\left(U_1^2 - C_0^2\right)k^2 + h_0\mathcal{R}\left(C_0 + U_2^2 - U_1^2\right)k^2|k| - h_0\frac{\tau}{\rho_1}k^4\right\} = 0,\end{aligned} \tag{4.37}$$

where we have put $C_0 = c_0 v_0$ and $\mathcal{R} = \frac{\rho_2}{\rho_1}$.

To make matters simpler, and to conform with what is done in Chapter 5, we will in the remainder of this section assume that $U_1 = 0$, and write $U_2 = U$. Applying this to (4.37) and completing the square yields the solutions

$$\omega = ck = h_0\mathcal{R}U|k|k \pm \left\{C_0^2k^2 - h_0\mathcal{R}(C_0^2 + U_2^2)|k|k^2 + h_0\frac{\tau}{\rho_1}k^4\right\}^{1/2}. \tag{4.38}$$

We see from the expression (4.38) that the solutions are stable only for U in the vicinity of C_0, as the sinusoidal waveforms (4.36) will feature exponential growth for imaginary values of c.

However, we can arrive at a different dispersion relation, one that conforms with the developments of Chapter (2). Recalling eq. (4.22) (this time with $U_1 = 0$), we can replace the system consisting of eqs. (4.33) and (4.34) with

$$gv_0^2\eta_x + w_t + ww_x + \mathcal{R}\mathcal{H}\left[h_0 w_{xt} + 2Uw_{xx} - U^2\eta_{xx}\right] - h_0\frac{\tau}{\rho_1}\eta_{xxx} = 0, \tag{4.39}$$

$$\eta_t + h_0 w_x + (w\eta)_x = 0. \tag{4.40}$$

With similar arguments like those leading to eq. (4.37), the dispersion relation for the system consisting of eqs. (4.39) and (4.40) is

$$\left\{1 + h_0\mathcal{R}|k|\right\}\omega^2 - 2\left\{h_0\mathcal{R}U|k|k\right\}\omega + \left\{h_0\mathcal{R}U^2|k|k^2 - C_0^2k^2 - h_0\frac{\tau}{\rho_1}k^4\right\} = 0, \tag{4.41}$$

which is the long-wave dispersion relation, eq. (2.19).

Chapter 5

Long wave dynamics for a liquid CO_2 lake in the deep ocean

This chapter presents our article to be submitted, in its complete form.

Long wave dynamics for a liquid CO_2 lake in the deep ocean

Krister J. Trandal* and Henrik Kalisch†

Abstract

A long-wave model for the evolution of long waves at the interface of a deep and a shallow fluid is put forward. The model allows for a uniform stream in one of the layers, and the existence of interfacial tension. The model can be used to study the dynamics of the interface between liquid CO_2 and seawater in the deep ocean, including the evolution of the hydrate layer.

If restricted to unidirectional waves the model has the form of a Benjamin-type equation found by Benjamin [1]. Steady periodic solutions of the Benjamin equation are found using a numerical bifurcation code based on a pseudo-spectral projection. The bifurcation patterns are complex, with some branches featuring turning points and secondary bifurcations.

KEYWORDS: interfacial waves, Kelvin-Helmholtz instability, liquid carbon-dioxide, deep ocean experiments

1 Introduction

In this paper, we study the motion of a free interface between two inviscid fluid layers in the presence of interfacial tension in the case when one of the fluids features a uniform flow parallel to the interface.

The motivation for this problem comes from recent suggestions that it might be possible to capture CO_2 from combustion processes, and sequester the CO_2 in the form of an underwater lake in the deep ocean [6, 12]. Given predominant oceanic temperatures, CO_2 condenses to the liquid phase at a pressure of about 4100 kPa, corresponding to a depth of about 400m [3, 10]. CO_2 in liquid form is still slightly compressible, and if it is located at about 3000m depth in the ocean, its density will be greater than that of seawater, and there is a possibility for stable storage in a large underwater depression (see Figure 1).

Since the density of the CO_2 is not much greater than that of seawater, the stability of the interface is a critical issue. Any large-scale perturbation of the interface might lead to bubbling up of CO_2 and over decades to eventual depletion of the underwater storage site.

As it turns out, CO_2 combines with H_2O to form an icelike solid known as hydrate, and the hydrate layer at the interface actually contributes to the stability of the interface. While it is sometimes modeled by including capillarity at the interface, recent experiments have shown that this approach to modeling the hydrate layer may not be appropriate as the hydrate layer is often broken into several pieces by strong wave motion. Nevertheless, significant efforts have been expended to evaluate the interfacial tension due to the hydrate layer. For example [14] reports on laboratory experiments under high pressure while [3] reports on wavetank experiments at 4000m depth designed to uncover the nature of the hydrate layer at large depth, and [7] investigates the strength of the capillarity in the deep-sea experiments.

*Department of Mathematics, University of Bergen, 5020 Bergen, Norway, krister.trandal@gmail.com
†Department of Mathematics, University of Bergen, 5020 Bergen, Norway, henrik.kalisch@uib.no

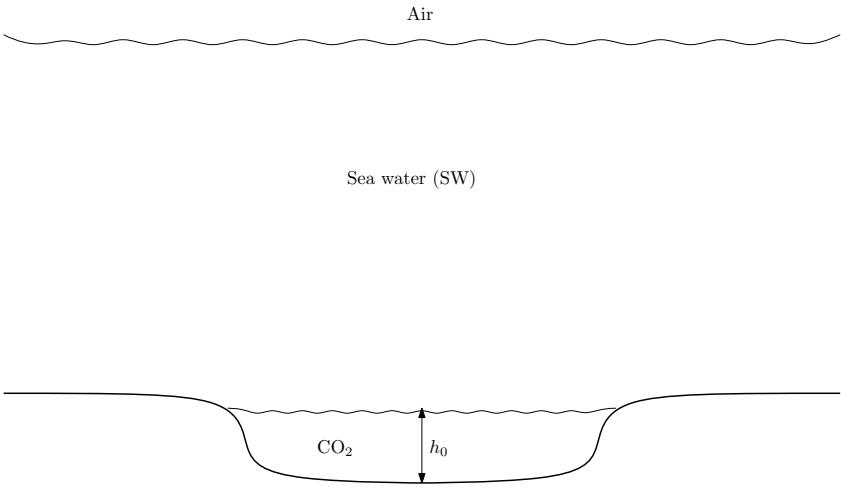

Figure 1: A lake of liquid CO_2 in a depression on the sea floor.

In the current work, we put forward a simple model equation which describes the wave motion at an interface between a shallow and a deep fluid. For the sake of being explicit, it is assumed that the upper layer is infinite, and features a background current.

We study the case of interfacial waves which are long when compared to the depth of the lower fluid. In this case, the problem is readily reduced to relatively simple model equations of Boussinesq type. The equations feature a non-local term which arises due to the large depth of the upper fluid. This dispersive term is in competition with the third-order term which originates from the inclusion of capillarity. In addition, there is a term which is due to the nonzero background stream of the upper fluid which is motivated by the modeling of bottom currents in the ocean.

Since the uniform stream in the upper layer drives waves predominantly in a single direction, it is natural to restrict the system to a unidirectional model. If this is done, a single model equation appears. The equation has the form

$$\eta_t + \eta_x + \frac{3}{2}\eta\eta_x - \beta\,\mathcal{H}\eta_{xx} - \gamma\,\eta_{xxx} = 0,$$

for certain values of β and γ which will be obtained in the body of the paper. As it turns out, this equation is similar to an equation found by Benjamin [1, 8], but the presence of the uniform flow in the upper fluid features prominently in one of the coeffifients. In order to solve this equation, we resort to a recently published open-source Python solver called `SpecTraVVave` [9]. In particular, we analyze the bifurcation diagram for steady solutions of the equation, and show that it features a number of interesting features such as turning points, secondary bifurcations and interconnected branches.

2 Problem formulation

The situation of study in this work will be a two-fluid system, separated by a sharp density interface located in the undisturbed state at $z = 0$ in a two-dimensional Cartesian xz-coordinate system. The fluids are assumed to have constant but possibly different densities, and the flow to be inviscid and irrotational in each layer. Furthermore, the velocity of the basic flow[1] is assumed

[1]We adopt the terminology from [4]. The term *basic flow* refers to the background flow that is present independent of interface deflection. The term *disturbed flow* then describes the flow that arise due to interface deflection. These two flows are superposed to give a total flow field. The potentials ψ and ϕ that appear represent the unknown disturbed flow field.

to be zero in the lower layer, while horizontal and uniform in the upper layer. See Figure 2 for a depiction along with a further description of the variables involved.

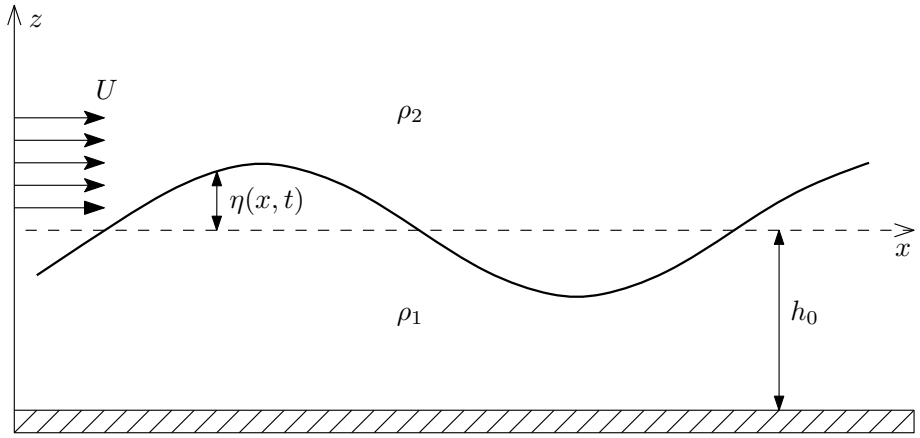

Figure 2: A schematic of the two-fluid interface problem. In the upper layer, with density ρ_2, there is an imposed horizontal shear velocity U. The upper layer is assumed to be infinitely deep while the lower layer, with density ρ_1, has finite, constant depth h_0. The function $z = \eta(x,t)$ represents the interface deflection at position x and time t. For visual clarity the wave amplitude is greatly exaggerated.

From the incompressible continuity equation and the assumption of irrotational flow, one will find that the velocity potential for each layer must satisfy Laplace's equation. That is,

$$\triangle\psi = 0 \quad \text{in} \quad \eta < z < \infty, \tag{1}$$

$$\triangle\phi = 0 \quad \text{in} \quad -h_0 < z < \eta, \tag{2}$$

together with the requirements that

$$\psi_x \to U, \quad \psi_z \to 0 \quad \text{if} \quad z \to \infty, \tag{3}$$

$$\phi_x = 0, \quad \phi_z = 0 \quad \text{at} \quad z = -h_0, \tag{4}$$

for the problem at hand. Conditions (3) state that the flow field should remain uniform far from the interface, while the conditions in eq. (4) are the no-slip and no flow-through boundary conditions, respectively. We assume that the variation in the transverse y-direction is negligible.

At the fluid interface, the following kinematic and dynamic boundary conditions are employed:

$$\left.\begin{aligned} \eta_t + (\psi_x + U)\eta_x &= \psi_z, && (5)\\ \eta_t + \phi_x\eta_x &= \phi_z, && (6)\\ p_1 - p_2 &= -\tau\eta_{xx}, && (7) \end{aligned}\right\} \quad \text{at} \quad z = \eta,$$

where p_1 and p_2 are the pressures in the fluid layers, measured close to the interface. The variable τ is the interfacial tension parameter. The dynamic boundary condition (7) may be rewritten with the help of a Bernoulli equation as

$$\rho_1\left(g\eta + \phi_t + \tfrac{1}{2}\phi_x^2 + \tfrac{1}{2}\phi_z^2\right) - \rho_2\left(g\eta + \psi_t + \tfrac{1}{2}\psi_x^2 + U\psi_x + \tfrac{1}{2}\psi_z^2\right) = \tau\,\eta_{xx}. \tag{8}$$

3 Derivation of the model equations

We now desire to derive a model system describing long-crested waves on fairly shallow water, and further restrict our attention to waves propagating in one direction on the interface between

two immiscible fluids. The subsequent derivation of the nonlinear equations is similar to the treatment given in [8] and [13, pp. 464-466].

3.1 Nondimensionalization

In order to make the assumptions on the geometry of the domain and the waves visible, and be able to deduce the relative order and importance of terms, we perform the following scaling on the variables:

$$\begin{aligned} z' &= \lambda Z \quad \text{in} \quad \eta' < z' < \infty, \\ z' &= h_0 z \quad \text{in} \quad -h_0 < z' < \eta', \end{aligned}$$

where original variables appear primed. Notice the different scaling used in the two fluid layers. Furthermore, we let

$$x' = \lambda x, \quad t' = \frac{\lambda}{c_0 v_0} t, \tag{9}$$

and

$$\eta' = a\eta, \quad \phi' = \frac{ag\lambda v_0}{c_0}\phi, \quad \psi' = \frac{ag\lambda v_0}{c_0}\psi, \tag{10}$$

where $c_0 = \sqrt{gh_0}$ is the limiting shallow water wave speed, and $v_0^2 = 1 - \frac{\rho_2}{\rho_1}$. We also introduce the parameters

$$\varepsilon = \frac{h_0}{\lambda}, \quad \sigma = \frac{a}{h_0}, \quad \mu = \frac{\tau}{(\rho_1 - \rho_2) g \lambda^2},$$

where ε, σ, μ are assumed to be small and of the same order. The parameter μ is similar to that of a reciprocal Bond number, and displays the relative importance of capillary effects versus gravity effects[2].

In normalized variables, the two kinematic boundary conditions (5), (6) are converted to

$$\eta_t + \left(\sigma \psi_x + \frac{U}{c_0 v_0} \right) \eta_x = \frac{1}{\varepsilon} \psi_Z, \tag{11}$$

$$\eta_t + \sigma \phi_x \eta_x = \frac{1}{\varepsilon^2} \phi_z. \tag{12}$$

The dynamic condition (8), after collecting terms and dividing out common factors, becomes

$$\eta + \phi_t + \frac{1}{2}\sigma\phi_x^2 + \frac{1}{2}\frac{\sigma}{\varepsilon^2}\phi_z^2 - \frac{\rho_2}{\rho_1}\left\{ \psi_t + \frac{1}{2}\sigma\psi_x^2 + \frac{1}{2}\sigma\psi_Z^2 + \frac{U}{c_0 v_0}\psi_x \right\} - \mu\eta_{xx} = 0. \tag{13}$$

3.2 Nonlinear system of equations

Subtracting eq. (12) from eq. (11) and rearranging, we get

$$\psi_Z = \frac{1}{\varepsilon}\phi_z + \varepsilon \frac{U}{c_0 v_0}\eta_x + \mathcal{O}(\varepsilon\sigma), \quad Z = \varepsilon\sigma\eta. \tag{14}$$

[2]The Bond number $\mathrm{Bo} = \frac{(\rho_1 - \rho_2) g L^2}{\tau}$, with L being a typical length scale, is not directly applicable here because the top layer has infinite depth (cf. [8, p. 171]).

In conjunction with the developments given in [13, pp. 460-466], we now desire to write a formal expansion for ϕ in powers of the vertical coordinate z, in our case about $z = -1$:

$$\phi = \sum_{n=0}^{\infty} (z+1)^n f_n(x,t).$$

Substitution into the normalized Laplace equation $\varepsilon^2 \phi_{xx} + \phi_{zz} = 0$ and the boundary condition $\phi_z(z=-1) = 0$ at the bottom of the lower layer give[3]

$$\phi = \sum_{n=0}^{\infty} (-1)^n \frac{\varepsilon^{2n}}{(2n)!} (z+1)^{2n} \frac{\partial^{2n}}{\partial x^{2n}} f(x,t) = f - \frac{1}{2}\varepsilon^2 (z+1)^2 f_{xx} + \mathcal{O}(\varepsilon^4),$$

where f_0 is now labeled f. This expression for ϕ gives

$$\phi_z = -\varepsilon^2 (z+1) f_{xx} + \mathcal{O}(\varepsilon^4). \tag{15}$$

Hence, from (14) we get

$$\psi_Z = -\varepsilon(1+\sigma\eta) f_{xx} + \varepsilon \frac{U}{c_0 v_0} \eta_x + \mathcal{O}(\varepsilon^2, \varepsilon\sigma), \quad Z = \varepsilon\sigma\eta. \tag{16}$$

We are then left with the Laplace equation for ψ. With the condition (16), the following elliptic problem appears

$$\begin{cases} \triangle \psi = 0, \quad Z > \varepsilon\sigma\eta, \\ \psi_Z = -\varepsilon(1+\sigma\eta) f_{xx} + \varepsilon \frac{U}{c_0 v_0} \eta_x + \mathcal{O}(\varepsilon^2, \varepsilon\sigma), \quad Z = \varepsilon\sigma\eta, \end{cases} \tag{17}$$

Expanding the boundary condition function ψ_Z in a Taylor series about $Z = 0$ allows the problem (17) to be shifted to the more tractable half-plane problem

$$\begin{cases} \triangle \psi = 0, \quad Z > 0, \\ \psi_Z = -\varepsilon f_{xx} + \varepsilon \frac{U}{c_0 v_0} \eta_x + \mathcal{O}(\varepsilon^2, \varepsilon\sigma), \quad Z = 0. \end{cases} \tag{18}$$

The solution of this upper half-plane Neumann problem is given by

$$\psi = -\varepsilon \mathcal{H} \left(\partial_x^{-1} P(Z) \left[f_{xx} - \frac{U}{c_0 v_0} \eta_x \right] \right) + \mathcal{O}(\varepsilon^2, \varepsilon\sigma),$$

where $\mathcal{H}$ is the Hilbert transform, which is defined by

$$\mathcal{H}[f](x) = \text{p.v.} \frac{1}{\pi} \int_{-\infty}^{\infty} \frac{f(x-y)}{y} \, dy,$$

with p.v. denoting the Cauchy principal value. Throughout this paper, the Hilbert transform is taken in the spatial variable $x \in \mathbb{R}$. The notation $P(\cdot)$ signifies a Poisson integral operator for the upper half-plane. Furthermore, we obtain

$$\psi(Z=0) = -\varepsilon \mathcal{H} \left(f_x - \frac{U}{c_0 v_0} \eta \right) + \mathcal{O}(\varepsilon^2, \varepsilon\sigma),$$

[3] All the terms of odd power vanish by virtue of the bottom layer boundary condition.

and

$$\psi_x(Z=0) = -\varepsilon\mathcal{H}\left(f_{xx} - \frac{U}{c_0 v_0}\eta_x\right) + \mathcal{O}(\varepsilon^2, \varepsilon\sigma).$$

To briefly summarize, we have that, at the interface

$$\phi_t = f_t + \mathcal{O}(\varepsilon^2), \quad \phi_x = f_x + \mathcal{O}(\varepsilon^2), \quad \phi_z = -\varepsilon^2(1+\sigma\eta)f_{xx},$$
$$\psi_t = -\varepsilon\mathcal{H}\left(f_{xt} - \frac{U}{c_0 v_0}\eta_t\right) + \mathcal{O}(\varepsilon^2, \varepsilon\sigma), \psi_x = -\varepsilon\mathcal{H}\left(f_{xx} - \frac{U}{c_0 v_0}\eta_x\right) + \mathcal{O}(\varepsilon^2, \varepsilon\sigma), \quad \psi_Z = \mathcal{O}(\varepsilon).$$

Substitution of these expressions into the normalized dynamic condition (13) gives

$$\eta + f_t + \frac{1}{2}\sigma f_x^2 + \varepsilon\frac{\rho_2}{\rho_1}\mathcal{H}\left(f_{xt} - \frac{U}{c_0 v_0}\eta_t + \frac{U}{c_0 v_0}f_{xx} - \frac{U^2}{c_0^2 v_0^2}\eta_x\right) - \mu\eta_{xx} = \mathcal{O}(\varepsilon^2, \varepsilon\sigma, \sigma^2, ...).$$

Differentiating with respect to x and writing $w = f_x$ yields

$$\eta_x + w_t + \sigma w w_x + \varepsilon\frac{\rho_2}{\rho_1}\mathcal{H}\left(w_{xt} - \frac{U}{c_0 v_0}\eta_{xt} + \frac{U}{c_0 v_0}w_{xx} - \frac{U^2}{c_0^2 v_0^2}\eta_{xx}\right) - \mu\eta_{xxx} = \mathcal{O}(\varepsilon^2, \varepsilon\sigma, \sigma^2, ...). \tag{19}$$

From this, it is evident that $\eta_x + w_t = \mathcal{O}(\varepsilon, \mu, \sigma)$. Assuming that differentiation and the application of $\mathcal{H}$ does not alter this order relation (cf. [8, p. 172]), we have

$$\mathcal{H}w_{xt} = -\mathcal{H}\eta_{xx} + \mathcal{O}(\varepsilon, \mu, \sigma). \tag{20}$$

Also, from the kinematic condition (12),

$$\eta_t + \sigma(w + \mathcal{O}(\varepsilon^2))\eta_x + (1+\sigma\eta)w_x + \mathcal{O}(\varepsilon^2) = 0.$$

This gives $\eta_t + w_x = \mathcal{O}(\varepsilon^2, \sigma)$ and, under the same assumptions leading to (20),

$$\mathcal{H}\eta_{xt} = -\mathcal{H}w_{xx} + \mathcal{O}(\varepsilon^2, \sigma). \tag{21}$$

Substitution of (20) and (21) into (19) results in

$$\eta_x + w_t + \sigma w w_x + \varepsilon\frac{\rho_2}{\rho_1}\mathcal{H}\left(2\frac{U}{c_0 v_0}w_{xx} - \eta_{xx} - \frac{U^2}{c_0^2 v_0^2}\eta_{xx}\right) - \mu\eta_{xxx} = \mathcal{O}(\varepsilon^2, \varepsilon\sigma, \sigma^2, ...)$$

Neglecting terms of quadratic and higher order in ε, σ and μ, we obtain the system

$$\begin{cases} \eta_x + w_t + \sigma w w_x + \varepsilon\frac{\rho_2}{\rho_1}\left(\frac{2U}{c_0 v_0}\mathcal{H}w_{xx} - \mathcal{H}\eta_{xx} - \frac{U^2}{c_0^2 v_0^2}\mathcal{H}\eta_{xx}\right) - \mu\eta_{xxx} = 0, \\ \eta_t + w_x + \sigma(\eta w)_x = 0. \end{cases} \tag{22}$$

Changing back to dimensional variables, the model system (22) becomes

$$\begin{cases} g v_0^2\eta_x + w_t + w w_x + \frac{\rho_2}{\rho_1}\left(2U h_0\mathcal{H}w_{xx} - c_0^2 v_0^2\mathcal{H}\eta_{xx} - U^2\mathcal{H}\eta_{xx}\right) - \frac{\tau}{\rho_1}\eta_{xxx} = 0, \\ \eta_t + h_0 w_x + (\eta w)_x = 0. \end{cases} \tag{23}$$

3.3 Unidirectional wave propagation

As mentioned our desire is to derive a model for waves propagating in one direction, so let us restrict our attention to waves propagating to the right. The nondimensional system (22) will serve as the outset for our development. To find solutions to first order in ε, σ and μ we propose the ansatz (cf. [8, p. 173])

$$w = \eta + \varepsilon A + \sigma B + \mu C$$

where A, B and C are functions of η and its derivatives. Substituting this expression into the nondimensional system (22) and disregarding higher order terms, we get

$$\begin{cases} \eta_t + \eta_x + \varepsilon \left[A_t - \frac{\rho_2}{\rho_1} \left(\frac{U}{c_0 v_0} - 1 \right)^2 \mathcal{H}\eta_{xx} \right] + \sigma \left(B_t + \eta\eta_x \right) + \mu \left(C_t - \eta_{xxx} \right) = 0, \\ \eta_t + \eta_x + \varepsilon A_x + \sigma \left(B_x + 2\eta\eta_x \right) + \mu C_x = 0. \end{cases} \tag{24}$$

Because $A = A(\eta, \eta_t, \eta_x ....)$, we may replace A_t by $-A_x$ to quadratic order in ε, and similarly for B and C. Doing so, the system (24) becomes

$$\begin{cases} \eta_t + \eta_x + \varepsilon \left[-A_x - \frac{\rho_2}{\rho_1} \left(\frac{U}{c_0 v_0} - 1 \right)^2 \mathcal{H}\eta_{xx} \right] + \sigma \left(-B_x + \eta\eta_x \right) + \mu \left(-C_x - \eta_{xxx} \right) = 0, \\ \eta_t + \eta_x + \varepsilon A_x + \sigma \left(B_x + 2\eta\eta_x \right) + \mu C_x = 0, \end{cases} \tag{25}$$

after higher order terms have been neglected. For consistency between the equations in (25), we require

$$\begin{aligned} A_x &= -A_x - \frac{\rho_2}{\rho_1} \left(\frac{U}{c_0 v_0} - 1 \right)^2 \mathcal{H}\eta_{xx}, \\ B_x + 2\eta\eta_x &= -B_x + \eta\eta_x, \\ C_x &= -C_x - \eta_{xxx}, \end{aligned}$$

which after rearrangement and integration gives

$$A = -\frac{1}{2} \frac{\rho_2}{\rho_1} \left(\frac{U}{c_0 v_0} - 1 \right)^2 \mathcal{H}\eta_x, \quad B = -\frac{1}{4}\eta^2, \quad C = -\frac{1}{2}\eta_{xx}.$$

Consequently,

$$w = \eta - \varepsilon \frac{1}{2} \frac{\rho_2}{\rho_1} \left(\frac{U}{c_0 v_0} - 1 \right)^2 \mathcal{H}\eta_x - \frac{1}{4}\sigma\eta^2 - \frac{1}{2}\mu\eta_{xx}.$$

Substituting this expression for w into the second equation in (22) and dropping quadratic terms, we obtain the model equation

$$\eta_t + \eta_x + \sigma \frac{3}{2}\eta\eta_x - \varepsilon \frac{1}{2} \frac{\rho_2}{\rho_1} \left(\frac{U}{c_0 v_0} - 1 \right)^2 \mathcal{H}\eta_{xx} - \mu \frac{1}{2}\eta_{xxx} = 0. \tag{26}$$

In equation (26), the quantities ε, σ and μ are unknown (they contain the unknown wave parameters a and λ). To circumvent this issue for the purpose of studying the equation numerically, we will subsequently return to dimensional variables and from there apply a second normalization. The model equation (26) in dimensional variables takes the form

$$\frac{1}{c_0 v_0}\eta_t + \eta_x + \frac{1}{h_0}\frac{3}{2}\eta\eta_x - h_0 \frac{1}{2} \frac{\rho_2}{\rho_1} \left(\frac{U}{c_0 v_0} - 1 \right)^2 \mathcal{H}\eta_{xx} - \frac{1}{2} \frac{\tau}{(\rho_1 - \rho_2)g}\eta_{xxx} = 0. \tag{27}$$

We now apply a normalization similar to that given in [2]. As before, original variables appear with a prime.

$$x' = h_0 x, \quad z' = h_0 z, \quad \eta' = h_0 \eta, \quad t' = \frac{h_0}{c_0 v_0} t.$$

Substituting these expressions into (27) and applying the chain rule of differentiation, we finally arrive at the model equation

$$\eta_t + \eta_x + \frac{3}{2}\eta\eta_x - \beta\,\mathcal{H}\eta_{xx} - \gamma\,\eta_{xxx} = 0, \tag{28}$$

where

$$\beta = \frac{1}{2}\frac{\rho_2}{\rho_1}\left(\frac{U}{c_0 v_0} - 1\right)^2, \quad \gamma = \frac{1}{2}\frac{\tau}{(\rho_1 - \rho_2) g h_0^2}. \tag{29}$$

4 Numerical method

In this section, the numerical procedure for approximating traveling wave solutions of eq. (28) is presented. The scheme is a spectral collocation method combined with a numerical continuation procedure for solving the nonlinear algebraic system that arise, and is implemented in a Python-based solver called `SpecTraVVave`. We will here elucidate the main features of the numerical method used in the package, briefly repeating what is presented in [9] to make the current discussion comprehensive. More details on workflow and class descriptions can be found in the source just cited and in the online repository [11].

4.1 Preamble

The package `SpecTraVVave` is written to tackle nonlinear dispersive equations of the general form

$$u_t + \big[f(u)\big]_x + \mathcal{L}[u_x] = 0, \tag{30}$$

where $\mathcal{L}$ is a linear, self-adjoint operator, and $f : \mathbb{R} \to \mathbb{R}$ satisfies $f(0) = f'(0) = 0$, in addition to some growth conditions [9, p. 3]. Furthermore, we regard $\mathcal{L}$ as a Fourier multiplier operator. That is,

$$\widehat{\mathcal{L}[u]}(\xi) = \alpha(\xi)\widehat{u}(\xi). \tag{31}$$

Our model equation (28) falls into this category, with

$$f(u) = \frac{3}{4}u^2, \quad \mathcal{L} = 1 - \beta\,\mathcal{H}\,\partial_x - \gamma\,\partial_x^2, \tag{32}$$

where β and γ are as defined in (29). The so-called flux function f and the multiplier function (or *symbol*) α are needed to run the solver. Using that $\widehat{\partial_x u}(\xi) = i\xi\widehat{u}(\xi)$, and $\widehat{\mathcal{H}u}(\xi) = -i\,\mathrm{sgn}(\xi)\widehat{u}(\xi)$ (cf. [9, p. 2]), it is not difficult to derive that

$$\alpha(\xi) = 1 - \beta|\xi| + \gamma\xi^2 \tag{33}$$

for the model equation (28).

4.2 Spectral collocation

The material presented here is analogous to that found in [9] and in [5]. As mentioned in the latter citation, since $\mathcal{L}$ is a Fourier multiplier operator, it is ideal to use a Fourier basis in the spectral method. The cited literature cover models like the Whitham equation, the Benjamin-Ono equation and the Benjamin equation. Our model equation is a type of Benjamin equation [1].

We are interested in computing traveling wave solutions of (30), i.e. solutions in the form

$$u(x,t) = \phi(w), \quad w = x - ct. \tag{34}$$

Substitution into (30) and applying the chain rule gives

$$-c\frac{d\phi}{dw} + \frac{d}{dw}\left[f(\phi)\right] + \mathcal{L}\frac{d\phi}{dw} = 0. \tag{35}$$

Integrating once with respect to w yields

$$-c\phi + f(\phi) + \mathcal{L}\phi = B, \tag{36}$$

where B is a constant of integration.

We will further restrict our attention to even periodic solutions of (30). As pointed out in [9, p. 3] this allows us to use a cosine collocation instead of a collocation founded on a more general Fourier basis. Also, because our solutions are even, the method will only need to compute half a solution profile, with the other half constructed by virtue of symmetry.

To be specific regarding the spectral projection, we desire to find approximate solutions in the space

$$\mathcal{S}_N = \operatorname{span}_{\mathbb{R}}\left\{\cos(\kappa_l x)\colon \kappa_l = \tfrac{2\pi}{L}l,\ 0 < l < N-1\right\} \subset L^2(0,L). \tag{37}$$

The domain is discretized with the collocation points

$$x_n = \frac{L}{2}\frac{2n-1}{2N}, \quad 1 \le n \le N. \tag{38}$$

We then look for a function $\phi_N \in \mathcal{S}_N$ satisfying the equation

$$-c\,\phi_N(x_n) + f(\phi_N)(x_n) + \mathcal{L}^N[\phi_N](x_n) = 0 \tag{39}$$

at each collocation point x_n, yielding a nonlinear algebraic system of N equations in N unknowns,

$$F\left(\phi_N, c\right) = 0, \quad F\colon \mathbb{R}^{N+1} \to \mathbb{R}^N, \tag{40}$$

which can be solved using Newton's method. As ϕ_N is a linear combination of cosines, i.e.

$$\phi_N(x) = \sum_{l=0}^{N-1} \zeta_l \cos(\kappa_l x), \tag{41}$$

its coefficients ζ_l can be computed using the discrete cosine transform (DCT), yielding

$$\zeta_0 = \frac{1}{N}C_0, \quad \zeta_l = \frac{2}{N}C_l, \quad l = 1, ..., N-1, \tag{42}$$

where the DCT $\{C_l\}_{l=0}^{N-1}$ consists of

$$C_l := \sum_{n=0}^{N-1} \phi_N(x_{n+1}) \cos\left(\frac{\pi}{2N}(2n+1)l\right) = \sum_{n=1}^{N} \phi_N(x_n)\cos(\kappa_l x_n), \quad l = 0, ..., N-1.$$

In (39), $\mathcal{L}^N$ is a discrete version of the operator $\mathcal{L}$. Because $\mathcal{L}$ is linear, and because eq. (39) is enforced at the N collocation points, we can evaluate the terms $\mathcal{L}^N[\phi_N](x_n)$ using matrix multiplication. More specifically, we have that

$$\mathcal{L}^N[\phi_N](x_i) = \sum_{j=1}^{N} \mathcal{L}^N(i,j)\phi_N(x_j), \tag{43}$$

where $\mathcal{L}^N(i,j)$ is the matrix defined by

$$\mathcal{L}^N(i,j) = \frac{1}{N}\alpha(0) + \frac{2}{N}\sum_{l=1}^{N-1} \alpha(\kappa_l)\cos(\kappa_l x_i)\cos(\kappa_l x_j). \tag{44}$$

In (44), $\alpha(\cdot)$ is the Fourier multiplier function of the operator $\mathcal{L}$, as defined in eq. (31).

4.3 Numerical continuation and bifurcation branch navigation

`SpecTraVVave` employs a continuation procedure to compute the next solutions of the system (46) and navigate the bifurcation branches. To deal with turning points on the bifurcation curve, both the phase speed and the wave amplitude are assumed to be depending on some parameter, say

$$a = a(\theta), \quad c = c(\theta). \tag{45}$$

The parameter θ is unknown and is to be computed from the extended nonlinear system

$$F\begin{pmatrix} \phi_N(x_1) \\ \phi_N(x_2) \\ \vdots \\ \phi_N(x_N) \\ B \\ \theta \end{pmatrix} = \begin{pmatrix} -c\,\phi_N(x_1) + f(\phi_N)(x_1) + \mathcal{L}^N[\phi_N](x_1) - B \\ -c\,\phi_N(x_2) + f(\phi_N)(x_2) + \mathcal{L}^N[\phi_N](x_2) - B \\ \vdots \\ -c\,\phi_N(x_N) + f(\phi_N)(x_N) + \mathcal{L}^N[\phi_N](x_N) - B \\ \Omega\left(\phi_N, a, c, B\right) \\ \phi_N(x_1) - \phi_N(x_N) - a \end{pmatrix} = \begin{pmatrix} 0 \\ 0 \\ \vdots \\ 0 \\ 0 \\ 0 \end{pmatrix} \tag{46}$$

In the system (46), $\Omega(\phi_N, a, c, B)$ is the boundary condition, and the `SpecTraVVave` package offers several choices that can be employed. For our study, we will employ the so-called `Mean()` boundary condition. That is, the condition that the mean of a solution be zero over the region of interest. This choice has roots in the physics of the problem: The mean of a solution profile over, say, a wavelength will have to be zero due to mass conservation (no fluid leaving the lower region, and interface is initially at rest). The numerical continuation works in a *predictor-corrector* fashion. From two successive points on the bifurcation curve,

$$P_1 = (c_1, a_1), \quad P_2 = (c_2, a_2),$$

i.e. two solutions of (46), we compute the direction vector

$$\mathbf{d} = (c_2 - c_1, a_2 - a_1) = (d^c, d^a). \tag{47}$$

We proceed to an initial guess P_3 for the next solution by moving a small increment s from P_2 in the direction $\mathbf{d}$:

$$P_3 = P_2 + s \cdot \mathbf{d} = (c_2 + s \cdot d^c, a_2 + s \cdot d^a). \tag{48}$$

This is the prediction step. Further, we require the solution P_* to lay on the line orthogonal to the one spanned by $\mathbf{d}$:

$$P_* = P_3 + \theta \cdot \mathbf{d}_\perp = \left(c_3 + \theta \cdot d^c_\perp, a_3 + \theta \cdot d^a_\perp\right), \quad d^c_\perp = -d^a, \quad d^a_\perp = d^c. \tag{49}$$

5 Results and concluding remarks

In the special case when $U = c_0 v_0$, our derived model equation (28) reduces to the KdV-type equation

$$u_t + u_x + \frac{3}{2} u u_x - \gamma u_{xxx} = 0, \tag{50}$$

which is well-known for being an exactly integrable equation, with solitary wave solutions

$$u(x,t) = 2(c-1)\,\mathrm{sech}^2\left(\frac{1}{2}\sqrt{\frac{1-c}{\gamma}}(x - ct - x_0)\right). \tag{51}$$

Having an exact solution at our disposal, it is desirable to test the accuracy of the numerical routine. Table 1 summarizes our findings. As can be seen the convergence is rather quick, in fact

grid size	$\log_{10}(\|\|u_{\text{exact}} - u\|\|)_{L^2}$	$\log_{10}(\|\|u_{\text{exact}} - u\|\|)_{L^\infty}$	Ratio of successive L^2 errors
32	-2.30473	-1.55271	
64	-3.39842	-2.50547	12.407
128	-6.98265	-6.06670	3839.085

Table 1: Errors for the KdV equation.

exponential, with increasing grid size.

We then did multiple runs of different values for the shear velocity U, with a wide range of admissible wave numbers (corresponding for the most part to positive speed c). A plot like that in Figure 3(a) was not uncommon, showing three terminating and connecting bifurcation brances, and the wave profiles at the points of connection. As can be seen, the profiles overlap, giving evidence to secondary bifurcations. The KdV case $U = c_0 v_0$ did not display such behavior, but values close to the critical value of $c_0 v_0$ did show terminating branches.

It was then natural to pose the question of whether this is unique behavior for the KdV-type equation, i.e. that the non-termination of branches is a closed condition to the KdV case. Investigating this issue further, our numerical findings point to a conclusion of a closed condition, but we believe that this should be substantiated further, with more runs closer to the critical value. One issue is then numerical accuracy regarding the computation of the constant β. Figure 4 shows the case $U = c_0 v_0 + 0.1$.

A Evaluation of the surface tension parameter

A quantification of the surface tension parameter τ will now be given. To get an initial approximation, we assume that instabilities are mainly due to short waves. The short wave dispersion relation can be shown to be

$$c = \frac{\rho_2 U}{\rho_1 + \rho_2} \pm \frac{1}{(\rho_1 + \rho_2)k}\left\{(\rho_1 + \rho_2)\tau k^3 - \rho_1\rho_2 U^2 k^2 + (\rho_1^2 - \rho_2^2) g k\right\}^{\frac{1}{2}} \tag{52}$$

Recalling that the interface Fourier modes are assumed to be of the form $\eta = \eta_0 e^{i(kx-\omega t)} = \eta_0 e^{ik(x-ct)}$, it is clear that imaginary values of c yield solutions with exponential growth. To avoid this, we require that the discriminant from the approximate expression (52) satisfies

$$D_{\text{approx}}(k) := (\rho_1 + \rho_2)\tau k^2 - \rho_1\rho_2 U^2 k + (\rho_1^2 - \rho_2^2) g > 0. \tag{53}$$

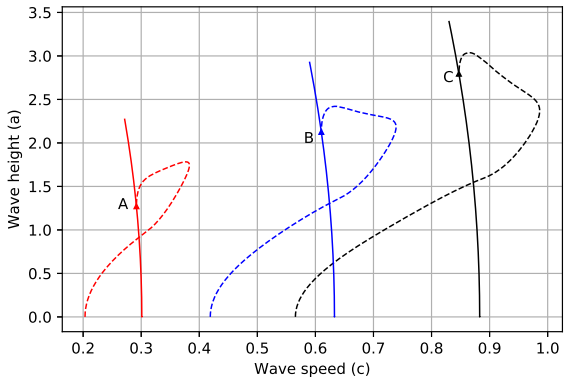

(a) Three points of bifurcation branch termination.

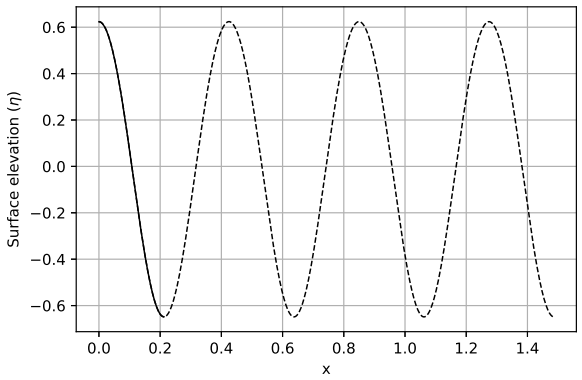

(b) Wave profiles at the connection point A, for wave numbers $k_3 = 1.85$ (dashed) and $k_3^* = 14.79997$ (solid).

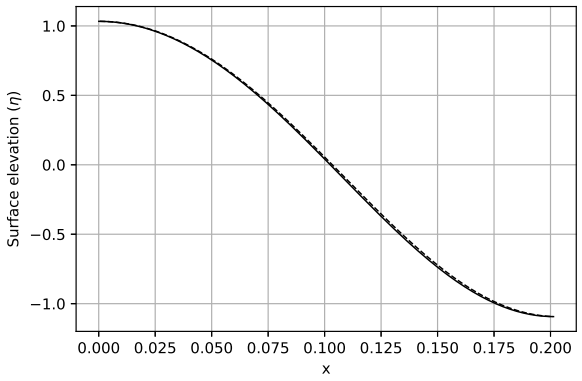

(c) Wave profiles at the connection point B, for wave numbers $k_2 = 1.30$ (dashed) and $k_2^* = 15.60001$ (solid). This plot is zoomed in, to give an enhanced view of the overlapping profiles.

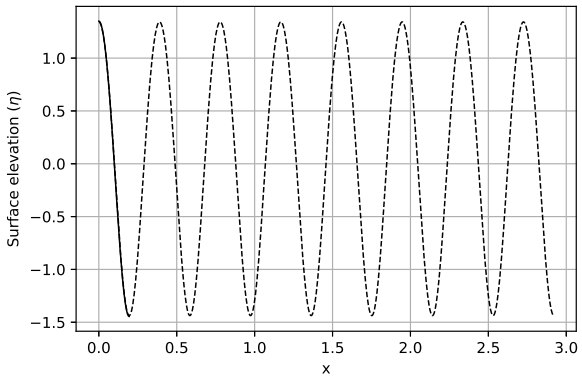

(d) Wave profiles at the connection point C, for wave numbers $k_1 = 0.95$ (dashed) and $k_1^* = 16.15004$ (solid).

Figure 3: Multiple connecting bifurcation curves for shear velocity $U = 2c_0v_0$, with wave profile at each point of connection. The branches connect at the points $A = (0.2918, 1.271)$, $B = (0.6102, 2.126)$ and $C = (0.8471, 2.795)$

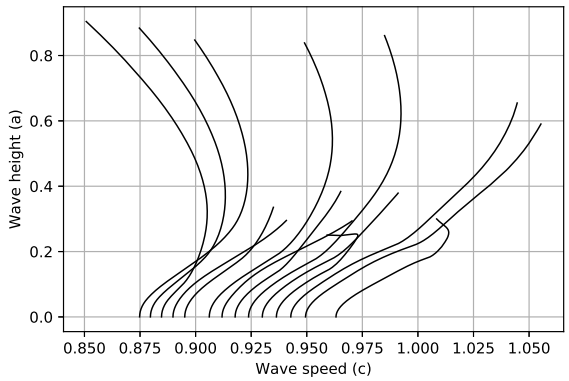

(a) Two curves can be seen turning, on their way to a termination point.

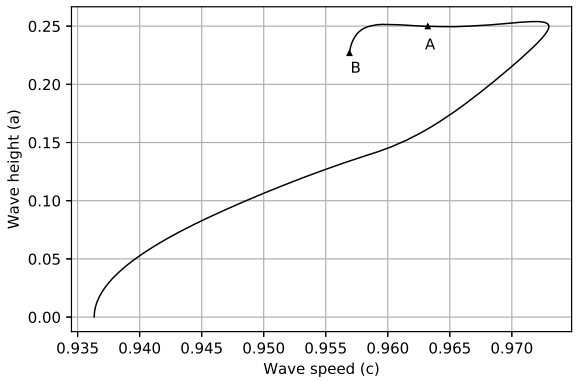

(b) A close-up on one of the turning branches in panel (a). Point A on the branch has approximate coordinates (0.963, 0.250), and B has approximate coordinates (0.957, 0.227).

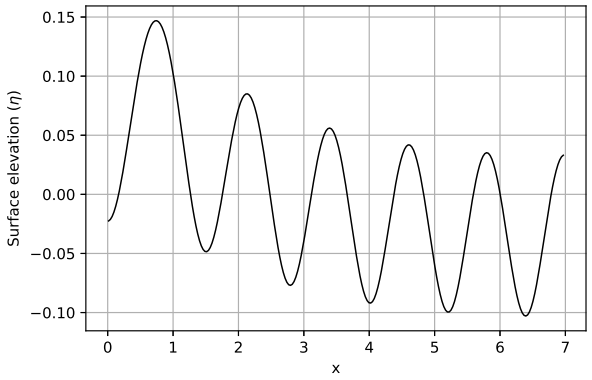

(c) Solution profile at the point A.

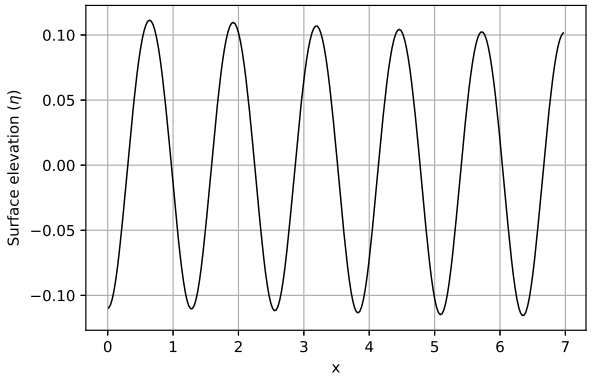

(d) Solution profile at the point B. One can see on the rather uniform profile that a termination point is being approached.

Figure 4: Bifurcation branches and selected solution profiles for the case $U = c_0 v_0 + 0.1$, with wave numbers running from 0.05 to 1.00.

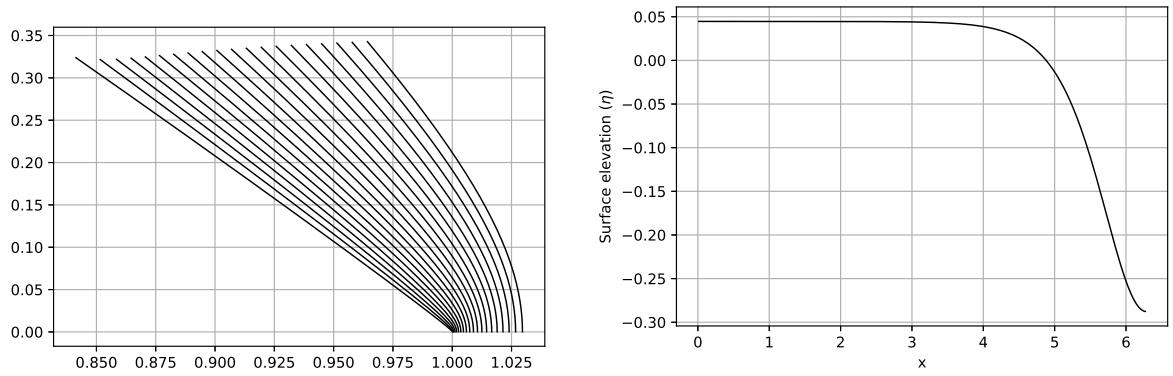

(a) Typical bifurcation branch plot for the KdV case $U = c_0 v_0$, with wave numbers ranging from 0.05 to 1.00.

(b) Typical KdV solution at the end of the branch corresponding to $k = 0.5$.

Figure 5: Bifurcation branches and solution profiles for the KdV-type equation. No turning or terminating curves are present.

Differentiating $D_{\text{approx}}(k)$ with respect to k, we find that (53) holds true if

$$\tau = \frac{\rho_1^2 \rho_2^2 U^4}{4(\rho_1 + \rho_2)(\rho_1^2 - \rho_2^2) g}. \tag{54}$$

An investigation of a deep ocean experiment with a CO_2 pool lowered to about 4000 m was carried out in [7]. From a conducted thruster experiment the authors studied the dynamics of the CO_2-seawater interface, specifically how it responded to various shear flow velocities. It was found that at a thruster setting yielding a critical shear velocity $U_c = 17.6$ cm/s, the interface became turbulent.

Using the critical velocity $U = U_c$, in addition to the values from Table 2, we find from eq. (54) that $\tau \approx 0.21$. This approximate value for τ may be used further in the full dispersion relation to obtain a more accurate approximation to the interfacial surface tension. This time, instead of differentiating the discriminant in the dispersion relation, denoted by $D(k)$, we wrote a Python program to find a value for τ that makes $\min_k D(k)$ positive and close to zero. Our finding is that

$$\tau \approx 0.22003$$

Parameter	Value	Units	Description
g	9.81	m/s^2	acceleration of gravity
h_0	0.11	m	lower layer depth (cf. [7])
ρ_1	1077.0	kg/m^3	lower layer density (cf. [7])
ρ_2	1045.7	kg/m^3	upper layer density (cf. [3])
U_c	0.176	m/s	critical shear velocity (cf. [7])

Table 2: Physical parameters and their values.

References

[1] T. B. Benjamin. A new kind of solitary wave. *Journal of Fluid Mechanics*, 245:401–411, 1992.

[2] H. Borluk and H. Kalisch. Particle dynamics in the KdV approximation. *Wave Motion*, 49:691–709, 2012.

[3] P. G. Brewer, E. T. Peltzer, P. Walz, I. Aya, K. Yamane, R. Kojima, Y. Nakajima, N. Nakayama, P. Haugan, and T. Johannessen. Deep ocean experiments with fossil fuel carbon dioxide: Creation and sensing of a controlled plume at 4 km depth. *J. Mar. Res.*, 63:9–33, 2005.

[4] P. G. Drazin and W. H. Reid. *Hydrodynamic stability*. Cambridge University Press, 2nd edition, 2004.

[5] M. Ehrnström and H. Kalisch. Global bifurcation for the Whitham equation. *Math. Mod. Nat. Phenomena*, 8:13–30, 2013.

[6] I. Fer and P. Haugan. Dissolution from a liquid CO_2 lake disposed in the deep ocean. *Limnol. Oceanogr.*, 48:872–883, 2003.

[7] P. M. Haugan and J. Hove. Dynamics of a CO_2-seawater interface in the deep ocean. *Journal of Marine Research*, 63:563–577, 2005.

[8] H. Kalisch. Derivation and comparison of model equations for interfacial capillary-gravity waves in deep water. *Mathematics and Computers in Simulation*, 74:168–178, 2007.

[9] H. Kalisch, D. Moldabayev, and O. Verdier. A numerical study of nonlinear dispersive wave models with SpecTraVVave. *Electronic Journal of Differential Equations*, 2017(62):1–23, 2017.

[10] Y. Kobayashi. Physical behavior of liquid CO_2 in the ocean. In *Direct Ocean Disposal of Carbon Dioxide*, pages 165–181. 1995.

[11] D. Moldabayev, O. Verdier, and H. Kalisch. SpecTraVVave. `http://github.com/olivierverdier/SpecTraVVave`, November 2016.

[12] K. Nealson. Lakes of liquid CO_2 in the deep sea. *Proc. Natl. Acad. Sci. U.S.A.*, 103:13903–13904, 2006.

[13] G. B. Whitham. *Linear and Nonlinear Waves*. Wiley, 1999.

[14] K. Yamane, I. Aya, S. Namie, and H. Nariai. Strength of CO_2 hydrate membrane in sea water at 40 MPa. *Ann. N.Y. Acad. Sci.*, 912:254–260, 2000.

Appendix A

Selected results from complex analysis

Here we list some well-known key results from complex analysis. The results are presented without proofs; the reader may consult [2] for such details. The cited literature is the source from which the results have been drawn. Before presenting the results, let us set the problem geometry in its own definition.

Definition A.1 (Geometry)**.** *Let $z = x + iy \in \mathbb{C}$, and*

$$\begin{aligned}
\mathcal{C}_0 &= \{z \colon z = R_0 e^{i\theta},\, 0 \leq \theta \leq 2\pi,\, R_0 > 0\},\\
\mathcal{C}_R &= \{z \colon z = R e^{i\phi},\, 0 \leq \phi \leq \pi,\, R > 0\},\\
\mathcal{C}_\rho &= \{z \colon z = x_0 + \rho e^{i\alpha},\, 0 \leq \alpha \leq \pi,\, x_0 \in \mathbb{R}\},\\
\mathcal{L}_1 &= (-R, x_0 - \rho) \subset \mathbb{R},\\
\mathcal{L}_2 &= (x_0 + \rho, R) \subset \mathbb{R},
\end{aligned}$$

where $R_0 < R$, and ρ is such that $\mathcal{C}_\rho$ is interior to $\mathcal{C}_R$. All contours except C_ρ are assumed to be oriented counter-clockwise.

See Figure A.1 for a depiction of these curves in the complex plane.

Theorem A.1 (Cauchy-Goursat theorem[1])**.** *Let $f(z)$ be a holomorphic function on and interior to a simple closed contour $\mathcal{C}$. Then we have that*

$$\int_{\mathcal{C}} f(z)dz = 0.$$

[1] An alternative name is Cauchy's integral theorem (not to be confused with Cauchy's integral formula, which is a different result, and hence a reason we are sticking to our title).

Lemma A.1 (Jordan's lemma)**.** *Let $f(z)$ be a holomorphic function in the upper half-plane $y \geq 0$ exterior to $\mathcal{C}_0$. Further, assume that there is a constant M_R such that*

$$\big|f(z)\big| \leq M_R \text{ and } \lim_{R\to\infty} M_R = 0,$$

for all points z on $\mathcal{C}_R$. Then

$$\lim_{R\to\infty} \int_{\mathcal{C}_R} f(z)e^{iaz}dz = 0,$$

for every $a > 0$.

Theorem A.2 (Indented paths)**.** *[2, p. 277] Assume that $f(z)$ has a Laurent series representation in a neighborhood of the simple pole $z = x_0 \in \mathbb{R}$, except possibly at x_0, and assume $\mathcal{C}_\rho$ (as given in Definition A.1) is contained in this neighborhood. Then*

$$\lim_{\rho\to 0} \int_{\mathcal{C}_\rho} f(z)dz = -\operatorname*{Res}_{z=z_0} f(z)\pi i.$$

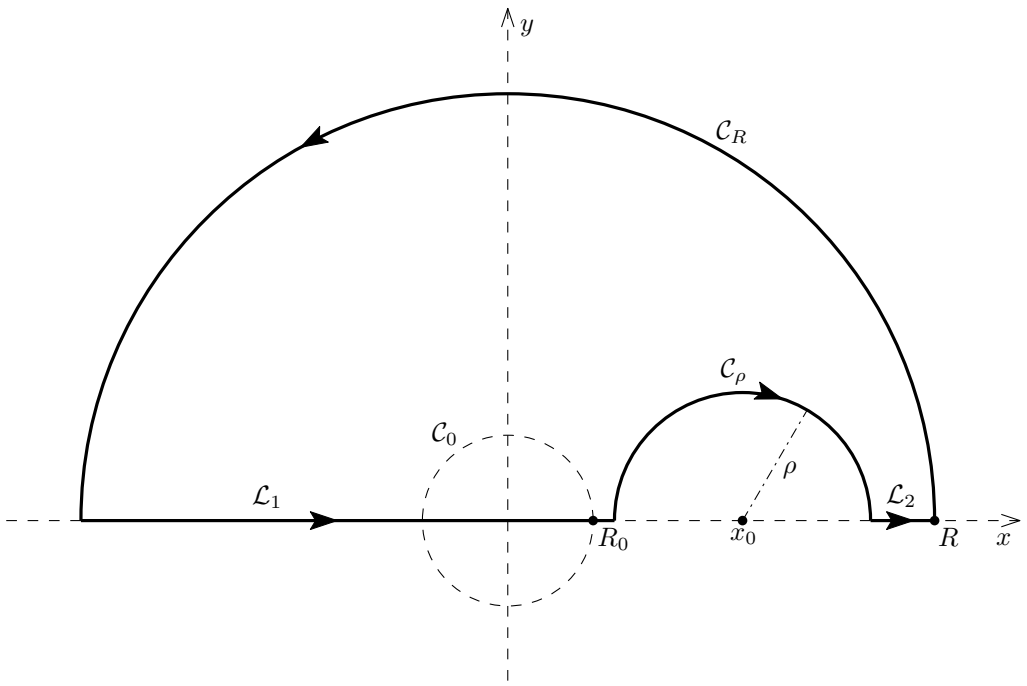

Figure A.1: Geometry from Definition A.1.

Appendix B

Source code

Main part of the Python code for computing the interfacial tension tau (see Chapter 5):

```
step = 0.0001
tolerance = 0.00001
last_distance = float("inf")

while True:
    tau += step

    discr = (tau*(rho1*1/np.tanh(h0*k) + rho2)*(k**3)
    - rho1*rho2*(U**2)*1/np.tanh(h0*k)*k**2
    + (rho1 - rho2)*(rho1*1/np.tanh(h0*k) + rho2)*g*k)

    distance = abs(discr.min())

    if distance < tolerance:
        break

    if distance > last_distance:
        tau -= step
        step = -step * 0.5

    last_distance = distance
```

Bibliography

[1] M. J. Ablowitz. *Nonlinear Dispersive Waves: Asymptotic Analysis and Solitons*. Cambridge University Press, 2011.

[2] J. W. Brown and R. W. Churchill. *Complex Variables and Applications*. McGraw-Hill, 8th edition, 2009.

[3] W. Cheney. *Analysis for Applied Mathematics*. Springer-Verlag, 2001.

[4] I. M. Cohen and P. K. Kundu. *Fluid Mechanics*. Academic Press, 4th edition, 2008.

[5] P. G. Drazin and R. S. Johnson. *Solitons: an introduction*. Cambridge University Press, 1989.

[6] P. G. Drazin and W. H. Reid. *Hydrodynamic stability*. Cambridge University Press, 2nd edition, 2004.

[7] M. Ehrnström and H. Kalisch. Global bifurcation for the Whitham equation. *Math. Mod. Nat. Phenomena*, 8:13–30, 2013.

[8] L. C. Evans. *Partial Differential Equations*. American Mathematical Society, 2nd edition, 2010.

[9] P. M. Haugan and J. Hove. Dynamics of a CO_2-seawater interface in the deep ocean. *Journal of Marine Research*, 63:563–577, 2005.

[10] H. Kalisch. Derivation and comparison of model equations for interfacial capillary-gravity waves in deep water. *Mathematics and Computers in Simulation*, 74:168–178, 2007.

[11] H. Kalisch, D. Moldabayev, and O. Verdier. A numerical study of nonlinear dispersive wave models with SpecTraVVave. *Electronic Journal of Differential Equations*, 2017(62):1–23, 2017.

[12] F. W. King. *Hilbert Transforms*, volume 1. Cambridge University Press, 2009.

[13] M. Klingspor. Hilbert transform: Mathematical theory and applications to signal processing. Master's thesis, University of Linköping, 2015.

[14] H. Lamb. *Hydrodynamics*. Cambridge University Press, 6th edition, 1932.

[15] J. Makhoul. A fast cosine transform in one and two dimensions. *IEEE Transactions on Acoustics, Speech, and Signal Processing*, ASSP-28(1):27–34, 1980.

[16] J. N. Reddy. *An Introduction to Continuum Mechanics*. Cambridge University Press, 2nd edition, 2013.

[17] R. S. Strichartz. *A Guide to Distribution Theory and Fourier Transforms*. World Scientific, 2003.

[18] G. B. Whitham. *Linear and Nonlinear Waves*. Wiley, 1999.